

# We are IntechOpen, the world's leading publisher of Open Access books Built by scientists, for scientists

4,800

Open access books available

122,000

International authors and editors

135M

Downloads

Our authors are among the

154

Countries delivered to

TOP 1%

most cited scientists

12.2%

Contributors from top 500 universities



WEB OF SCIENCE™

Selection of our books indexed in the Book Citation Index  
in Web of Science™ Core Collection (BKCI)

Interested in publishing with us?  
Contact [book.department@intechopen.com](mailto:book.department@intechopen.com)

Numbers displayed above are based on latest data collected.  
For more information visit [www.intechopen.com](http://www.intechopen.com)



# Structural and Calorimetric Studies of Zinc, Magnesium and Manganese Based Phosphate and Phosphate-Silicate Glasses

*Refka Oueslati Omrani, Mohamed Jemal, Ismail Khattech and Ahmed Hichem Hamzaoui*

## Abstract

Glasses of the  $(50-x/2)\text{Na}_2\text{O}-x\text{MO}-(50-x/2)\text{P}_2\text{O}_5$  ( $M = \text{Zn, Mg or Mn}$ ) ( $0 \leq x \leq 33$  mol%),  $(50-x)\text{Na}_2\text{O}-x\text{MO}-50\text{P}_2\text{O}_5$  ( $M = \text{Zn, Mn}$ ) ( $0 \leq x \leq 33$  mol%), and  $(0.9-x)\text{NaPO}_3-x\text{SiO}_2-0.1\text{ZnO}$  ( $0 \leq x \leq 0.1$  mol) were prepared by the melt quenching technique. Samples were investigated by means of X-ray diffraction, Archimede's method, ellipsometry, Fourier-transformed infrared (FTIR), Raman,  $^{31}\text{P}$  solid state magic angle spinning nuclear magnetic resonance (MAS-NMR), UV-visible spectroscopy and calorimetry. For zinc, manganese and magnesium phosphate glasses, the increase in density with the addition of MO oxide suggests the compactness of the vitreous network. For zinc phosphate silicate glasses, the variations of density and refractive index were attributed to the structural changes when  $\text{SiO}_2$  oxide is progressively introduced. The increase in the glass transition temperature ( $T_g$ ) reflects an increase in the cross-link strength of the structure as MO and  $\text{SiO}_2$  oxides are gradually incorporated. For all glass composition, spectroscopic investigations revealed the depolymerization of metaphosphate chains ( $Q^2$ ) allowing the formation of phosphate dimers ( $Q^1$ ). Calorimetric dissolution shows that the dissolution is endothermic for lower MO content and become exothermic when  $x$  rises. For  $(50-x/2)\text{Na}_2\text{O}-x\text{ZnO}-(50-x/2)\text{P}_2\text{O}_5$  ( $0 \leq x \leq 33$  mol%) glasses, the formation enthalpy increases with the incorporation of ZnO oxide.

**Keywords:** phosphate glasses, phosphate-silicate glasses, depolymerization, modifier oxide, calorimetric dissolution, formation enthalpy, thermochemical cycle

## 1. Introduction

Over the past several decades, great interests have been considered for phosphate glasses due to their superior physical properties which impart them a several advantages over conventional silicate and borate glasses.

Phosphate-based glasses are an interesting class in the world of glass and glass ceramics owing to their higher thermal expansion, lower melting and softening

temperature, higher ultra-violet transmission and optical characteristic. Phosphate glasses have potential of applications in medicine, biology, batteries, laser technology, electronic, telecommunication [1–44].

In recent times, phosphate glasses have received considerable interest as a result of the synthesis of new glass composition with high chemical stability. The improvement of this quality induces the application of phosphate glasses in numerous fields of materials science, such as fast ionic conductors, semiconductors, photonic materials, hermetic seals, rare-earth in host solid state lasers and biomedical materials [1–44].

Thus, phosphate and silicate glasses are the most important materials which can extensively be used for laser sources and fiber amplifiers [3].

The basic structure unit of the phosphate network is based on corner-sharing  $PO_4$  units which form chains and rings or isolated groups  $PO_4$  [6].

The covalence of the bridging oxygen atoms is responsible for the formation of phosphate groups [18, 27].

The structure of the three dimensional network is obtained by linking three oxygen atoms with others  $PO_4$  tetrahedrons. The metaphosphate groups contain two covalent bridging oxygen atoms. Whereas, the pyrophosphate groups are formed by bending only single oxygen atom with other tetrahedral site.

Recently, the structure of phosphate glass is describes using the O/P ratio [13, 18, 19, 27]. Furthermore, many investigators used the O/P ratio in order to classify the distribution of phosphate groups in the vitreous network. **Table 1** reports the classification of phosphate glasses as a function of O/P ratio [45].

For  $2.5 < O/P < 3$ , the glass network is described by the distribution of ultraphosphate groups [19].

The metaphosphate groups are obtained for O/P ratio equal to 3. The glass network is described by the connection of  $PO_4$  tetrahedral anions with neighbors in order to form chains and rings.

For polyphosphate glasses, the O/P ratio is between 3 and 3.5. The structure is described by chains formed by  $PO_4$  tetrahedral anions joined with others.

For  $O/P = 3.5$ , the structure is obtained by forming the phosphate dimers such as pyrophosphate groups in which two  $PO_4$  tetrahedral shared one bridging oxygen [19]. For  $3.5 < O/P < 4$ , the isolated  $PO_4^{3-}$  units are formed such as orthophosphate.

The increase of O/P ratio induces the depolymerization of phosphate groups which suggests the shortening of the average chain length [19].

The network connectivity of phosphate compound is conventionally expressed as  $Q^n$  tetrahedral sites ( $n = 0...3$ ), when  $n$  is the number of bridging oxygen (BO) per  $Q$  unit to neighbor phosphate tetrahedral [2, 23, 28].  $Q^0$  represents orthophosphates ( $PO_4^{3-}$ ),  $Q^3$  is pure  $P_2O_5$  and  $Q^2$  (metaphosphates) and  $Q^1$  (pyrophosphates)

O/P	Classification	$Q^n$
2.5-3	Ultraphosphates	$Q^3$
3	Metaphosphates	$Q^2$
>3	Polyphosphates	$Q^2 + Q^1$
3.5	Pyrophosphates	$Q^2$
>3.5	Orthophosphates	$Q^0$
O: oxygen atom	P: Phosphorus atom	Q: Phosphorus tetrahedral sites

**Table 1.** Classification of phosphate glasses as a function of O/P ratio and  $Q_n$  tetrahedral sites.

are intermediate structures [11, 13, 16, 19, 20]. **Figure 1a** shows the nomenclature of phosphate groups as  $Q^n$  tetrahedral sites also with the variation of an O/P ratio [45].

For silicon-oxygen networks,  $n$  varies between 0 and 4, where  $Q^0$  represents orthosilicates ( $SiO_4^{4-}$ ),  $Q^4$  is pure  $SiO_2$  and  $Q^3$ ,  $Q^2$  and  $Q^1$  represents the intermediate silicate structures [2, 20].

Glasses results from many possible combinations of network-forming oxides together with one or several modifier or intermediate oxides which lead to a special physical properties [22].

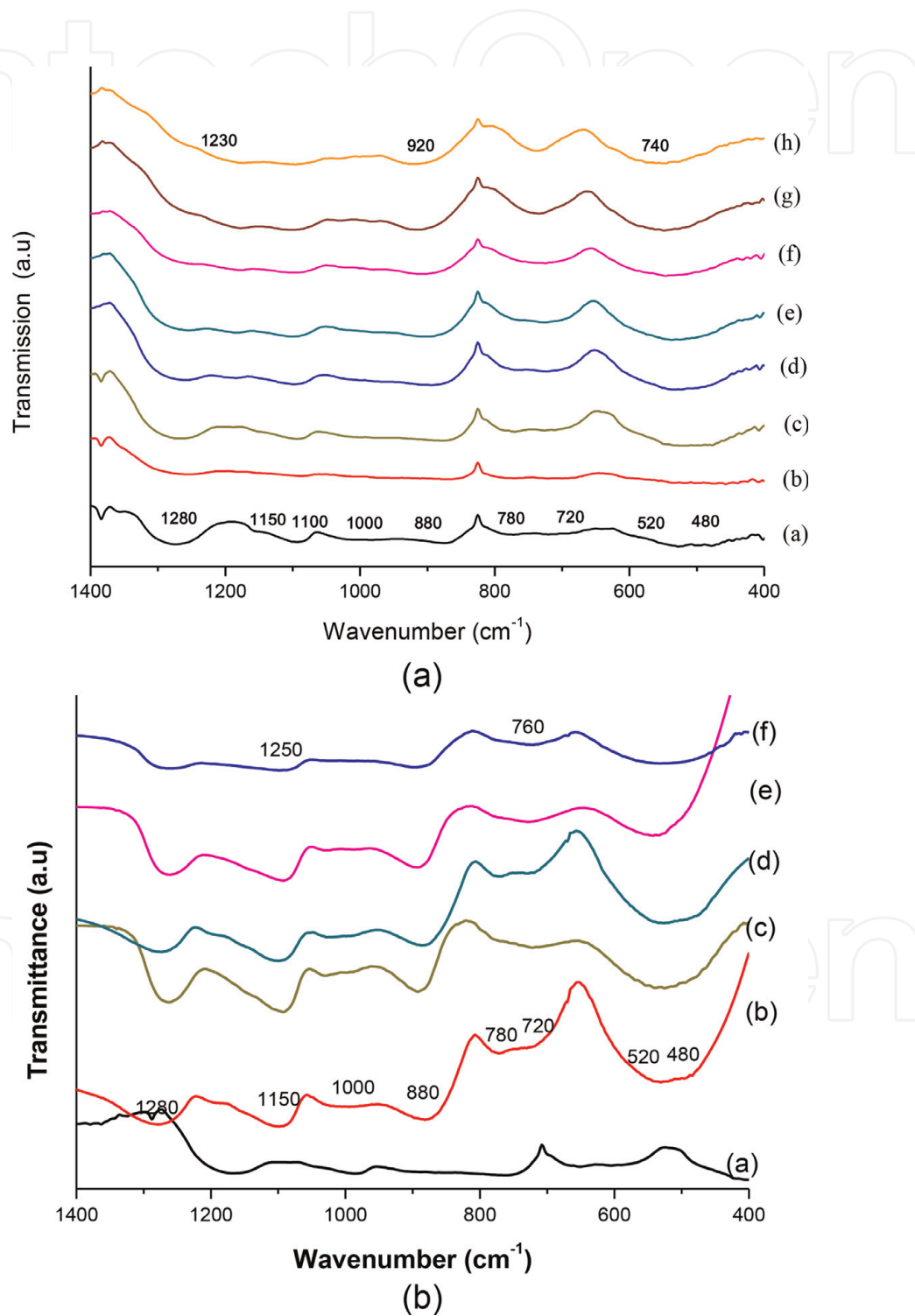


**Figure 1.**

*a. Infrared spectra of  $(50-x)Na_2O-xZnO-50P_2O_5$  glasses: (a) 0 mol% ZnO, (b) 5 mol% ZnO, (c) 10 mol% ZnO, (d) 15 mol% ZnO, (e) 20 mol% ZnO, (f) 25 mol% ZnO, (g) 30 mol% ZnO, (h) 33 mol% ZnO.*

*b. Infrared spectra of  $(0.9-x)NaPO_3-xSiO_2-0.1ZnO$  ( $0 \leq x \leq 0.1$  mol) glasses: (a) 0 mol  $SiO_2$ , (b) 0.02 mol  $SiO_2$ , (c) 0.04 mol  $SiO_2$ , (d) 0.06 mol  $SiO_2$ , (e) 0.08 mol  $SiO_2$ , (f) 0.10 mol  $SiO_2$ .*

Introducing alkali metal oxide or divalent metal oxide to the glass network induces the fundamental optical absorption edge falls in the UV region below 400 nm which meets with the requirement for desirable applications in optical systems [22]. These additions not only enhance the chemical durability of the phosphate glasses but also can impart special functions to the glasses and expand the glass application fields.

Furthermore, alkali phosphate glasses have attracted more attention due to their mixed electronic ionic conductivity, low melting point and strong glass-forming character [4]. Among the phosphate-based glasses those containing calcium, magnesium, sodium and zinc have received great attention due to their excellent optical properties, high refractive index, low dispersion and good transparency in the UV and IR region [1]. With the decrease of  $P_2O_5$  content, the glass become more resistant to moisture attack but restricts the glass formation areas. Thus, MgO oxide was incorporated in order to overcome these problems [23].

Nevertheless, phosphate-based glasses containing transition metal ions are scientifically interesting materials due to their attractive properties which can be used in many technological applications including electronic and electro-optical devices [21].

In fact, transition metal oxides can be dissolved easily in phosphate glasses which exhibit one than more oxidation states [21, 25, 30].

For glasses doped with manganese ions. These latter are presented in the +2 or +3 oxidation states. The content of  $Mn^{3+}$  ions in the glass leads to the staining glass in the color range from light to dark purple depending on the concentration [30]. This characteristic coloration could be explained by the d-d electronic transitions. This color can be associated with the broad absorption band in the visible region at 520 nm, which pertains to the  $Mn^{3+}$  ions [25, 30]. This behavior allows obtaining additional luminescence bands in the red spectral region that shift LED emission from cool white to warm light [30].

Contrary to  $Zn^{2+}$  and  $Mg^{2+}$  ions presented in one oxidation state, spectral-luminescent properties of manganese ions in phosphate glasses allow them to be good candidates for interesting optical applications [21, 25, 30].

In borate glasses, manganese exists mainly as  $Mn^{3+}$  ions with octahedral coordination in glass networks whereas in silicate and germanate glasses, it identified as  $Mn^{2+}$  ions with both tetrahedral and octahedral coordination [21].

Referring to literature, Montagne et al. have been studied the zinc phosphate glasses with a general formula  $(100-x)NaPO_3-xZnO$  with  $0 < x < 33.3$  mol% using  $^{31}P$  MAS-NMR,  $^{31}P$  NMR of liquid sample, visible spectroscopy, refractive index measurements, density evolutions,  $T_g$  variations, activation energy, chemical durability and chemical analysis [1, 2, 46, 47].

The obtained results revealed the distortion of metaphosphate chains ( $Q^2$ ) which suggests the formation of phosphate dimers ( $Q^1$ ) [46, 47].

Moreover, Zotov et al. have been studied the manganese phosphate glasses with a general formula  $(MnO)_x(NaPO_3)_{1-x}$  when  $x = 0.0, 0.024, 0.048$  and  $0.167$  mol [48].

These investigations have been performed using X ray diffraction, EXAFS and Raman spectroscopy. The increase of MnO content causes the depolymerization of metaphosphate chains leading to the decrease of the average chain length [48].

For zinc phosphate-silicate glasses, chemical compositions of the prepared glasses, picked from literature, have been chosen with higher level of  $SiO_2$  and lower  $P_2O_5$  content [2, 20, 24, 34].

Aguiar et al. have been studied the  $Na_2O-MgO-CaO-P_2O_5-SiO_2$  bioactive glasses using Raman,  $^{31}P$  MAS-NMR and  $^{29}Si$  MAS-NMR spectroscopies. The glass compositions were prepared with varying  $SiO_2$  content from 25 to 54 mol% and the  $P_2O_5$  proportion from 2 to 11 mol% [2, 20, 24].

Furthermore, Szumera et al. have detailed the effect of MoO<sub>3</sub> addition on silicate phosphate glasses using spectroscopic analysis such as FTIR, Raman and <sup>31</sup>P MAS-NMR. The molar content of SiO<sub>2</sub> decreases from 41.6 to 39.6 mol% and the P<sub>2</sub>O<sub>5</sub> proportion increases from 5.7 to 7.8 mol% [44]. The obtained results revealed the cleavage of oxygen bridges which suggests that acts as a network modifier [44].

In our knowledge, the thermochemical data of zinc-, magnesium-, and manganese-based phosphate and phosphate-silicate glasses are rare in literature. For this purpose, the aims of this research were to study the correlations between structural changes, thermal investigations, optical properties and thermochemical behaviors of these glassy compounds with the incorporation of zinc, magnesium and manganese oxides.

However, it is well known that phosphate glasses have a poor chemical durability, volatile nature and hygroscopic character. These disadvantages decrease their stability which limits their use in technological applications [5].

The addition of alkali and alkaline earth cations with the decrease of phosphorus content can depolymerize the glass network which suggests the cleavage of P—O—P bridges [28].

The incorporation of certain network modifier cations (Na<sup>+</sup>, K<sup>+</sup>, Mg<sup>+</sup>, Ca<sup>2+</sup>...) disrupts the glassy network, leading to the structure depolymerization and the formation of non-bridging oxygen atoms (NBO), also named terminal oxygen (O<sub>T</sub>) [2, 4].

The addition of transition metal oxides (CuO, MgO, ZnO, MnO, CaO...) into the vitreous network (TMO) disrupted the P—O—P bridges leading to the structure depolymerization and the formation of non-bridging oxygen atoms (NBO) [2, 5, 6, 8, 9, 13, 21, 25, 32, 35]. Which induces the formation of P—O—M bonds replacing the easily hydrosoluble P—O—P bridge that improve the chemical durability of the phosphate network [21].

Among several oxides mentioned above, zinc oxide gained considerable attention because Zinc doped glasses find numerous applications in optic field can be used as LED light sources and substrates for optical waveguides. It can also play an important role in bone formation and mineralization [3].

Zinc phosphate compositions are chemically durable, have processing temperatures under 400°C and can be co-formed with high temperature under 400°C polymers to produce unusual organic/inorganic composites [19].

In recent years, there have also appeared some publications on the influence of the addition of ZnO on the structure of glasses with a mixed phosphate-silicate structure [7, 34].

Among the wide class of phosphate glasses, ZnO-based glasses have low glass transition temperature in the region of 280–380°C and significantly high chemical durability [14].

Furthermore, the addition of ZnO to the glass network is expected to improve the chemical stability of the structure. It can also ameliorate the electrical, optical and magnetic properties of glasses due to the appearance of P—O—Zn ionic bond which induces the increase in the compactness and the rigidity of the glass network [5, 13, 32, 35].

In fact, in crystalline solid compound, the structure was described by a repetitive arrangement of a large scale patterns contrary to amorphous structure which exhibits a short range order.

Additionally, ZnO is an intermediate oxide. It can act as former or modifier network depending on his content in phosphate network. When it occupies the tetrahedral sites by forming ZnO<sub>4</sub> structural units, ZnO oxide plays the role of glass former. But, when it occupies the octahedral sites coordinated, ZnO oxide acts as glass modifier [7, 25].

The literature concerning zinc in various mixed oxide compounds revealed that with the exception of few structures, zinc has tetrahedral oxygen ligancy and the zinc-oxygen distance varies only slightly [25, 34]. It was concluded that zinc had a coordination number of six in borate and silicate glasses [34].

Interestingly, the heat treatment of glasses at temperature higher than their glass transition ( $T_g$ ) or crystallization temperature ( $T_c$ ) improves the electrical conductivity of the glassy compound due to the “structural relaxation” of the glass network [36].

ZnO is widely used in glass production because it improves the glass quality by enhancing mechanical properties and chemical durability and by reducing the thermal expansion [7]. Zinc is a microelement that plays an important role in the bone formation and mineralization. Zinc containing glasses and glass ceramics has been developed for bone engineering applications [7]. The small size of Zn ion (0.74 Å) helps it to locate itself into smaller cavities of the network [37].

Moreover, MgO oxide is of interest from a biological viewpoint because  $Mg^{2+}$  is known to play a physiological role in positively influencing bone strength which can be substituted into apatites [13, 18].

The bioactive behavior of magnesium rich glasses is identified as their ability to react chemically with living tissues, forming with them mechanically strong and lasting bonds. These bone bondings are attributed to the formation of an apatite-like layer on the glass surface, with composition and structure equivalent to the mineral phase of bone.

In fact, bioactive glasses have received special attention due to their better bone bonding ability *in vivo*. Due to their good bioactive and tailorable degradation properties, these glasses can be used for various biomedical applications such as bone graft, filler, dental, implant coating.

Furthermore, by increasing the concentration of modifier oxides, electrical conductivity of the glass increases. This property was probably influenced by the structural changes resulting from the disruption of the glass network which affected the mobility of the cations and anions when the modifying oxide was progressively introduced [38].

Glasses containing transition metal oxides possess interesting electronic, optic and magnetic properties due to the ability to exist in more than one valence state. However, the electronic conduction of these glassy compounds is resulting from the electronic transfer of cation that exists in different valence states [4, 38].

Compared with phosphate glasses, silicate glasses exhibit superior chemical resistance which makes them compatible with the fabrication process in the development of optical devices [3].

Silicate glasses are an attractive host matrix for transition metal ions due to their excellent optical and mechanical properties, good chemical durability, good chemical stability and low thermal expansion coefficient leading to strong thermal resistance [6]. Silicate glasses have many advantages rather than phosphate glasses. Silicate-based glasses are chemically durable, thermally stable and optically transparent at excitation and lasing wavelength. However, the higher viscosity of these glasses allows the glass to be formed without crystallization process. In addition, these amorphous materials are useful in optics as lenses or beam splitters in optical telecommunications, micro- and optoelectronics and in near IR-windows [6, 39, 40].

## **2. Experimental procedures**

### **2.1 Glass preparation**

Glasses of the  $(50-x/2)Na_2O-xMO-(50-x/2)P_2O_5$  ( $M = Zn, Mn, Mg$ ) ( $0 \leq x \leq 33$  mol%),  $(50-x)Na_2O-xMO-50P_2O_5$  ( $M = Zn, Mn$ ) ( $0 \leq x \leq 33$  mol%), and

$(0.9-x)\text{NaPO}_3-x\text{SiO}_2-0.1\text{ZnO}$  ( $0 \leq x \leq 0.1$  mol) compositions have been prepared using a melt quenching technique.

A series of glasses were prepared by varying the MO (M = Zn, Mn, Mg) content from 0 to 33 mol% using reagent grade compounds,  $\text{NaH}_2\text{PO}_4$ ,  $\text{NH}_4\text{H}_2\text{PO}_4$ , MgO, ZnO,  $\text{MnCO}_3$  with a high purity (99% purity), in the suitable proportions.

The mixture corresponding to the desired compositions was heated in platinum crucible at  $400^\circ\text{C}$  in order to evaporate water and start the condensation of phosphate groups. The temperature was then progressively increased to  $750-900^\circ\text{C}$ , depending on glass composition, and held constant for 30 min. The batch was finally quenched to room temperature under air atmosphere in order to produce vitreous compounds.

Using the same technique, phosphate-based silicate glasses with a general formula  $(0.9-x)\text{NaPO}_3-x\text{SiO}_2-0.1\text{ZnO}$  ( $0 \leq x \leq 0.1$  mol) have been synthesized using reagent grade compounds,  $\text{NaH}_2\text{PO}_4$ ,  $\text{H}_2\text{O}$ , ZnO and  $\text{SiO}_2$  with a high purity (99% purity) with the desired compositions.

The mixture was then putted in platinum crucible at  $400^\circ\text{C}$  for 1 hour in order to eliminate residual water. The temperature was raised progressively to  $1200^\circ\text{C}$  for 30 min in order to homogenize the melting mixture. Finally, the batch was quenched to room temperature under air atmosphere in order to obtain glasses.

The amorphous state was confirmed by X-ray diffraction. All the products were annealed at about  $20^\circ\text{C}$  below their glass transition temperature for 2 hours in order to eliminate internal tensions and get a more homogenized sample.

## 2.2 ICP analysis

Phosphorus, sodium, magnesium, zinc, manganese and silica were analyzed by inductively coupled plasma atomic emission spectroscopy (Jobin Yvon Ultra C).

## 2.3 Physical properties

### 2.3.1 Density and molar volume

Density of glass is a strong function of its composition and its intrinsic property which shed light on the short range structure of the glassy material [4, 37]. This work presents a series of glasses with various amounts of modifier oxides. These modifies, depending on their polarity and size, tend to occupy the interstices within the network and form new bonds resulting in a change in the structure and properties of the glass [4, 37].

Glass density measurements have been determined using the standard Archimedes method using diethyl orthophthalate as immersion fluid. The relative error of these measurements is  $\pm 3\%$ .

The molar volume of glasses has been calculated from the density ( $V_m = M/\rho$ ) and the molar weight.

For  $(50-x/2)\text{Na}_2\text{O}-x\text{MO}-(50-x/2)\text{P}_2\text{O}_5$  (M = Zn, Mn, Mg) where  $3 \leq \text{O/P} \leq 3.49$  and  $(50-x)\text{Na}_2\text{O}-x\text{MO}-50\text{P}_2\text{O}_5$  (M = Zn, Mn) with  $\text{O/P} = 3$  ( $0 \leq x \leq 33$  mol%) series glasses, the density increases gradually with the incorporation of MO oxide. The increase in density indicates that the MO oxide reticulate the vitreous network because  $\text{P}-\text{O}-\text{M}$  bond are more ionic than  $\text{P}-\text{O}-\text{P}$  [11-13, 15, 29, 32, 33, 42].

**Table 2** shows that the molar volume decreases monotonically with the increase of ZnO content for phosphate glasses.

The decrease in the molar volume for  $(50-x/2)\text{Na}_2\text{O}-x\text{MO}-(50-x/2)\text{P}_2\text{O}_5$  (M = Zn, Mn, Mg) where  $3 \leq \text{O/P} \leq 3.49$  and  $(50-x)\text{Na}_2\text{O}-x\text{MO}-50\text{P}_2\text{O}_5$  (M = Zn, Mn) with  $\text{O/P} = 3$  ( $0 \leq x \leq 33$  mol%) series glasses could be explained by the higher



field  $\Delta F$  ( $\Delta F = Z/r^2$ ; with  $z$  is the valence cation and  $r$  is the ionic radius) of  $M^{2+}$  compared to that of  $Na^+$  [11–13, 15, 29, 32, 33, 42].

The decrease in the molar volume is extensively related to structural changes due to the incorporation of MO oxide that disrupted the average chain length of metaphosphate resulting from the following reaction:



The variation of these properties is closely related to the structural modification when  $M^{2+}$  ion is progressively introduced.

The effect of composition on the density and molar volume for zinc phosphate-silicate glass, having a general formula:  $(0.9-x)NaPO_3-xSiO_2-0.1ZnO$  ( $0 \leq x \leq 0.1$  mol), shows that the replacement of  $NaPO_3$  by  $SiO_2$  oxide induces a decrease of density as mentioned **Table 3**. This is due to the lower molecular weight of  $SiO_2$  than that of  $NaPO_3$  ( $M_{SiO_2} = 60 \text{ gmol}^{-1}$ ,  $M_{NaPO_3} = 102 \text{ gmol}^{-1}$ ) [11–13, 15, 29, 32, 33, 42].

As the same for the molar volume, this quantity decreases monotonically with the incorporation of  $SiO_2$  oxide (**Table 3**). This variation indicates that  $SiO_2$  oxide reticulates the vitreous network suggesting the increase in the rigidity of the structure.

Furthermore, the regular decrease in the molar volume is closely related to the nature of bending in the glass structure, because  $P-O-Si$  are more ionic than  $P-O-P$  bridges, suggesting the compactness of the vitreous network [11–13, 15, 29, 32, 33, 42].

### 2.3.2 DSC investigations

Generally, the glass transition phenomenon occurs due to the increasing viscosity of the overcooled liquids so  $T_g$  strongly depends on the polymerization ratio of the network [40].

Glass composition	X	Density ( $\text{g cm}^{-3}$ )	$V_m$ ( $\text{cm}^3 \text{mol}^{-1}$ )	$T_g$ (°C)	$T_c$ (°C)	$\Delta T$ (°C)
$(50-x/2)Na_2O-xZnO-(50-x/2)P_2O_5$	0	$2.43 \pm 0.07$	$42.00 \pm 1.30$	$280 \pm 5$	$290 \pm 5$	10
	5	$2.47 \pm 0.07$	$41.00 \pm 1.23$	-	-	-
	10	$2.62 \pm 0.08$	$38.15 \pm 1.14$	$285 \pm 5$	$371 \pm 5$	86
	15	$2.70 \pm 0.08$	$36.63 \pm 1.10$	-	-	-
	20	$2.75 \pm 0.08$	$35.60 \pm 1.10$	$287 \pm 5$	$368 \pm 5$	81
	25	$2.85 \pm 0.09$	$34.00 \pm 1.02$	$294 \pm 5$	$439 \pm 5$	145
	30	$2.93 \pm 0.09$	$32.70 \pm 1.00$	$306 \pm 5$	$456 \pm 5$	150
	33	$2.98 \pm 0.09$	$32.00 \pm 1.00$	$314 \pm 5$	$446 \pm 5$	132

**Table 2.**

Density, molar volume, glass composition, glass transition temperature  $T_g$ ,  $T_c$ ,  $\Delta T$  of  $(50-x/2)Na_2O-xZnO-(50-x/2)P_2O_5$  ( $0 \leq x \leq 33$  mol%) phosphate glasses.

Glass composition	x	Density ( $\text{gcm}^{-3}$ )	$V_m$ ( $\text{cm}^3 \text{mol}^{-1}$ )	n	$T_g$ (°C)	$T_c$ (°C)	$\Delta T$ (°C)
$(0.9-x)NaPO_3-xSiO_2-0.1ZnO$	0	$2.60 \pm 0.10$	$38.50 \pm 1.20$	$1.44 \pm 0.05$	$280 \pm 5$	$371 \pm 5$	86
	0.02	$2.58 \pm 0.10$	$38.35 \pm 1.20$	$1.45 \pm 0.05$	$287 \pm 5$	$400 \pm 5$	113
	0.04	$2.57 \pm 0.10$	$38.24 \pm 1.20$	$1.46 \pm 0.05$	$289 \pm 5$	$427 \pm 5$	138
	0.06	$2.55 \pm 0.10$	$38.13 \pm 1.10$	$1.47 \pm 0.05$	$293 \pm 5$	$439 \pm 5$	146
	0.08	$2.55 \pm 0.10$	$38.00 \pm 1.10$	$1.48 \pm 0.05$	$294 \pm 5$	$475 \pm 5$	163
	0.1	$2.53 \pm 0.10$	$37.80 \pm 1.10$	$1.49 \pm 0.05$	$296 \pm 5$	$466 \pm 5$	170

**Table 3.**

Density, molar volume, refractive index, glass composition, glass transition temperature  $T_g$ ,  $T_c$ ,  $\Delta T$  of  $(0.9-x)NaPO_3-xSiO_2-0.1ZnO$  ( $0 \leq x \leq 0.1$  mol) glass series.

The glass transition temperatures were determined on 40–50 mg of samples using DSC-ATD Netzsch 404 PC with a 10°C/min heating rate (accuracy  $\pm 5^\circ\text{C}$ ).

With increasing MO content, glass transition temperature,  $T_g$ , increases linearly for all glass compositions as mentioned **Table 2**.

This behavior is undoubtedly corresponding to some changes in the nature of bonding in the structural network. This parameter is strictly related to the bond strength of the glass network which can be explained in terms of bond length (which is the charge divided by the square of the cation-oxygen distance) affected by the cation field strength resulting in a higher of  $T_g$  values [11–13, 15, 29, 32, 33, 42].

These variations indicate the progressive increase of the reticulation and the rigidity of the glass network by gathering the non-bridging oxygen atoms (NBO) with the increase of MO proportion. As a result the formation of P—O—M bonds suggesting the increase in the rigidity and the compactness of the structure that ameliorate the chemical durability of glasses.

A similar behavior has been observed for zinc phosphate-silicate glasses [11–13, 15, 29, 32, 33, 42].

According to Dietzel, the thermal stability of glasses ( $\Delta T$ ) can be expressed by the temperature difference between  $T_g$  and  $T_c$ ,  $\Delta T = T_c - T_g$ , in which  $T_g$  and  $T_c$  are the glass transition and crystallization temperature. Increasing  $\Delta T$  delays the nucleation process, indicating a better stability of the glass [29].

Inspecting these data, one can note that the undoped ZnO and SiO<sub>2</sub> oxide glass matrix has the lowest thermal stability indicating a tendency towards crystallization as shown **Tables 2 and 3**.

$\Delta T$  increases when SiO<sub>2</sub> oxide is progressively added, indicating a better stability of the glass. The larger value of  $\Delta T$ , the stronger is the inhibition to nucleation and crystallization process as mentioned **Table 3** [12, 13, 15, 29, 32, 33].

### 2.3.3 Refractive index measurements

The ability to control the physical properties of glasses, e.g., the refractive index, by variation in glass composition suggests the feasibility of chemically controlling the materials according to the needs of a given application [3].

For glassy compounds, refractive index is a fundamental parameter that strongly relevant to optical devices performance and reliability in the basic elements in all optical instruments. Hence, a large number of researchers have carried out investigations to ascertain the relation between refractive index and glass composition [10].

This parameter is one of the fundamental properties of materials, because it is closely related to the electric polarizability of ions and the local field inside the material [3, 10, 11].

The characteristic feature of phosphate glasses is the low value of the refractive index that is in the order of 1.49. The variation of this quantity for zinc phosphate-based silicate glasses is presented in **Table 4**. Inspecting these data, one can note that  $n$  increases from 1.44 to 1.49 when  $x$  rises from 0 to 10 mol% of SiO<sub>2</sub> oxide which suggests that the refractive index of glassy compounds depends essentially on the density of glass network [3, 10, 11].

In addition to density, many parameters can prevail the refractive index such as density, polarizability of the first neighbor ions coordinated with it (anion), coordination number of ion, electronic polarizability of the oxide ion and optical basicity [3, 10, 11]. The molar refractivity ( $R_m$ ) was estimated from the refractive index and the molar volume ( $V_m$ ) using the Lorenz-Lorenz Equation [3, 10, 11]:

$$R_m = \frac{(n^2 - 1)}{(n^2 + 2)} V_m \quad (2)$$

Glass composition	n	$\alpha_m$ (Å <sup>3</sup> )	$R_m$ (cm <sup>3</sup> mol <sup>-1</sup> )	$E_{opt}$ (ev)	$(\alpha_m/V_m) \times 10^{-25}$
0.9NaPO <sub>3</sub> -0.1ZnO	1.44	4.06	10.23	1.50	1.05
0.88NaPO <sub>3</sub> -0.02SiO <sub>2</sub> -0.1ZnO	1.45	4.07	10.30	1.70	1.06
0.86NaPO <sub>3</sub> -0.04SiO <sub>2</sub> -0.1ZnO	1.46	4.13	10.40	2.00	1.08
0.84NaPO <sub>3</sub> -0.06SiO <sub>2</sub> -0.1ZnO	1.47	4.15	10.50	2.25	1.09
0.82NaPO <sub>3</sub> -0.08SiO <sub>2</sub> -0.1ZnO	1.48	4.18	10.55	2.35	1.10
0.8NaPO <sub>3</sub> -0.1SiO <sub>2</sub> -0.1ZnO	1.49	4.20	10.60	2.35	1.11

**Table 4.** Refractive index, molar refractivity ( $R_m$ ), molar electronic polarizability ( $\alpha_m$ ) and band gap energy of (0.9-x) NaPO<sub>3</sub>-xSiO<sub>2</sub>-0.1ZnO ( $0 \leq x \leq 0.1$  Mol) glass series.

The molar electronic polarizability  $\alpha_m$  was calculated using the relation of Clasius-Mosotti as follows [3, 10, 11]:

$$\alpha_m = \frac{3}{4} \Pi N R_m \quad (3)$$

where the value of  $\frac{3}{4} \Pi N$  is known as the Lorentz function and N is the Avogadro number. **Table 4** reports the values of  $R_m$  and  $\alpha_m$ . These parameters increase gradually with the incorporation of SiO<sub>2</sub> oxide.

**Table 4** shows that  $R_m$  increases from 10.23 to 10.60 m<sup>3</sup> mol<sup>-1</sup> and  $\alpha_m$  are between 4.06 and 4.20 Å. These variations indicate that the refractive index as a function of both density and molar electric polarizability of glassy compounds [3, 10, 11].

In the present work, we found that the refractive index (n) depends on the ratio ( $\frac{\alpha_m}{V_m}$ ). This quantity shows that the refractive index (n) of the studied glasses increases linearly versus ( $\frac{\alpha_m}{V_m}$ ) ratio. This variation can be probably due to the electronic polarizability of oxide ions.

For Na<sub>2</sub>O ionic-based glasses, the polarizability of oxygen ions has the smaller value ( $\alpha_{O^{2-}} = 2.45$  Å) compared to copper rich glasses [3, 10, 11].

Duffy et al. suggested that increasing the optical basicity ( $\Lambda = 1.67 \left(1 - \frac{1}{\alpha_{O^{2-}}}\right)$ ) indicates an increase in the effective electronic density of the oxide ions and accordingly, increasing covalency in the oxygen-cation bonding [3, 10, 11].

The decrease in the molar volume for zinc-based phosphate-silicate glasses induces an increase in the rigidity and the compactness of the vitreous network, when SiO<sub>2</sub> oxide is progressively introduced, because Si—O—P bonds are more ionic than P—O—P.

## 2.4 Spectroscopic analysis

### 2.4.1 FTIR spectroscopy

Infrared spectra of the glass series have been recorded by Perkin-Elmer (FTIR 2000) spectrometer using KBr pellets in the frequency range 400–4000 cm<sup>-1</sup> at room temperature. The samples were prepared by grinding about 9 mg of glass powder with 300 mg of spectroscopic grade dried KBr.

For undoped zinc phosphate glasses, NaPO<sub>3</sub>, FTIR spectrum revealed an asymmetric and symmetric stretching vibration band of PO<sub>2</sub> groups in metaphosphate chains situated respectively at 1280 and 1150 cm<sup>-1</sup>. The asymmetric and symmetric stretching vibration bands of PO<sub>3</sub> chain end groups situated respectively at 1100 and 1000 cm<sup>-1</sup> [12, 13, 15, 29, 32, 33].

Furthermore, the asymmetric and symmetric stretching vibrations of P—O—P bands are around 880, 780 and 720  $\text{cm}^{-1}$ . The deformation mode of P—O—( $\text{PO}_4^{3-}$ ) groups at 535 and 480  $\text{cm}^{-1}$  [12, 13, 15, 29, 32, 33].

FTIR spectra of  $(50-x/2)\text{Na}_2\text{O}-x\text{ZnO}-(50-x/2)\text{P}_2\text{O}_5$  and  $(0.9-x)\text{NaPO}_3-x\text{SiO}_2-0.1\text{ZnO}$  glasses are shown in **Figures 1a** and **b**.

As MO oxide is introduced, the asymmetric band of  $\text{PO}_2$  shifts from 1280  $\text{cm}^{-1}$  shift to lower frequency as showed **Figures 1a** and **b** indicating the depolymerization of phosphate chains when  $x$  increases [12, 13, 15, 29, 32, 33].

For higher ZnO content, FTIR spectra revealed the displacement of the asymmetric stretching mode vibration of the P—O—P band from 880 to 920  $\text{cm}^{-1}$  when  $x$  rises from 0 to 33 mol%. This result can be correlated to the increase in the covalence character of P—O—P bridges when monovalent cation  $\text{Na}^+$  was replaced by divalent cation (such as  $\text{Zn}^{2+}$ ) [12, 13, 15, 29, 32, 33].

It may be also attributed to the shortening of phosphate chain length due to the higher field strength and the size of the metallic cation, when the ratio O/P increases for  $(50-x/2)\text{Na}_2\text{O}-x\text{ZnO}-(50-x/2)\text{P}_2\text{O}_5$  [12, 13, 15, 29, 32, 33].

The FTIR spectra of  $\text{NaPO}_3$  glasses revealed also two bands in the frequency range 780–720  $\text{cm}^{-1}$  which are attributed to the presence of two P—O—P bridges in metaphosphate chains based on  $(\text{P}_2\text{O}_6)^{2-}$  groups (**Figure 1a** and **b**) [12, 13, 15, 29, 32, 33]. However, it is interesting to note that for the series glasses containing 30 and 33 mol% ZnO FTIR spectra exhibit only a single band at 740  $\text{cm}^{-1}$  assigned to the P—O—P linkage in pyrophosphate group  $(\text{P}_2\text{O}_7)^{4-}$  (**Figure 1a**) [12, 13, 15, 29, 32, 33]. These spectral changes depend essentially on the glass composition.

On the other hand, this result could be explained by disruption of the infinite metaphosphate chains when MO oxide is gradually incorporated suggesting the depolymerization of the skeleton of  $(\text{P}_2\text{O}_6^{2-})_\infty$  into short phosphate groups such as:  $\text{P}_2\text{O}_7^{4-}$  and  $\text{PO}_4^{3-}$  [12, 13, 15, 29, 32, 33].

Similar FTIR spectra have been recorded for zinc phosphate-based silicate glasses, with a general formula:  $(0.9-x)\text{NaPO}_3-x\text{SiO}_2-0.1\text{ZnO}$ , ( $0 \leq x \leq 0.1$  mol) as mentioned **Figure 1b**.

The FTIR spectra of zinc phosphate-based silicate glasses revealed the appearance of some bands assigned to phosphate-silicate glasses in the range 1000–1300  $\text{cm}^{-1}$  as shown **Figure 1b**. The asymmetric stretching vibration bands of silicate and phosphate tetrahedron is located at 1100  $\text{cm}^{-1}$ . It seems that a smaller band at 840  $\text{cm}^{-1}$  is attributed to the symmetric stretching vibration of O—Si—O in metasilicate ( $\text{Q}^2$ ) when  $\text{SiO}_4$  tetrahedron shared two oxygen with their neighbor (Si—O—2NBO). The symmetric stretching vibration band Si—O—Si is about 1080  $\text{cm}^{-1}$ . In addition, the bending vibration of Si—O—Si and O—Si—O bonds is around 460  $\text{cm}^{-1}$  [12, 13, 15, 29, 32, 33].

When  $\text{SiO}_2$  is incorporated, FTIR spectra revealed the displacement of the asymmetric stretching mode vibration of  $\text{PO}_2$  band from 1280 to 1250  $\text{cm}^{-1}$  when  $x$  increases from 0 to 10 mol%. This result can be probably due to the depolymerization of the infinite metaphosphate chains with the addition of  $\text{SiO}_2$  oxide.

Furthermore, for 0.8  $\text{NaPO}_3-0.1\text{SiO}_2-0.1\text{ZnO}$  glass composition, FTIR spectrum revealed the appearance of a only a single band at 760  $\text{cm}^{-1}$  assigned to P—O—P bands in phosphate dimers  $(\text{P}_2\text{O}_7^{4-})$  as mentioned **Figure 1b**. These spectral changes have been observed for magnesium and manganese phosphate glasses that could be attributed to the reduction of infinite phosphate groups  $(\text{P}_2\text{O}_6^{2-})$  into shorter phosphate groups such as:  $\text{P}_2\text{O}_7^{4-}$  and  $\text{PO}_4^{3-}$  [12, 13, 15, 29, 32, 33].

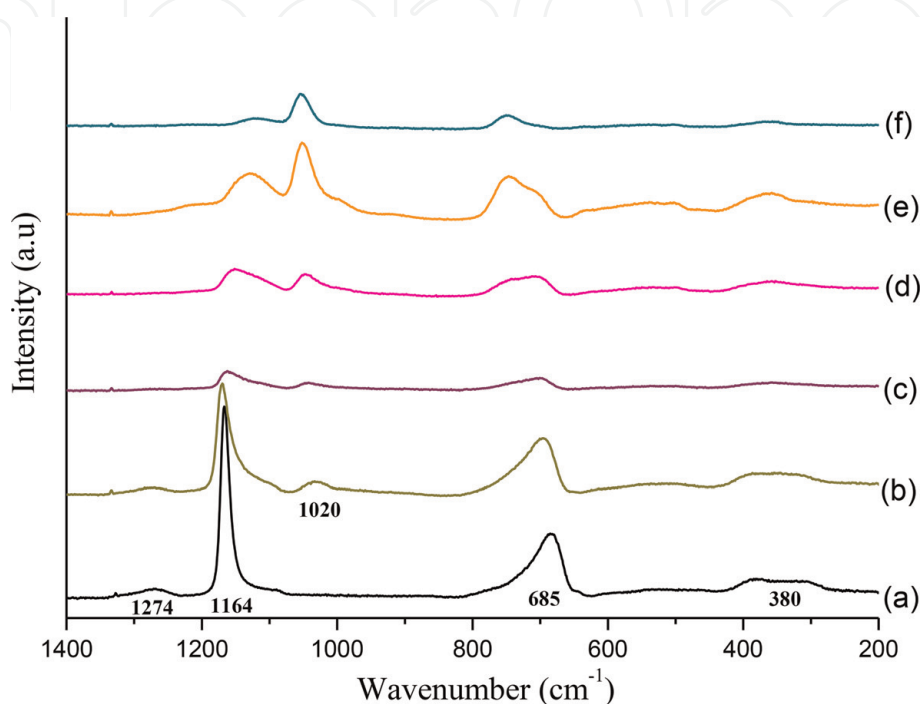
#### 2.4.2 Raman spectroscopy

Raman spectroscopy is an adequate technique for the analysis of glass matrix structure. Raman bands are generally characteristics of structures involving chains

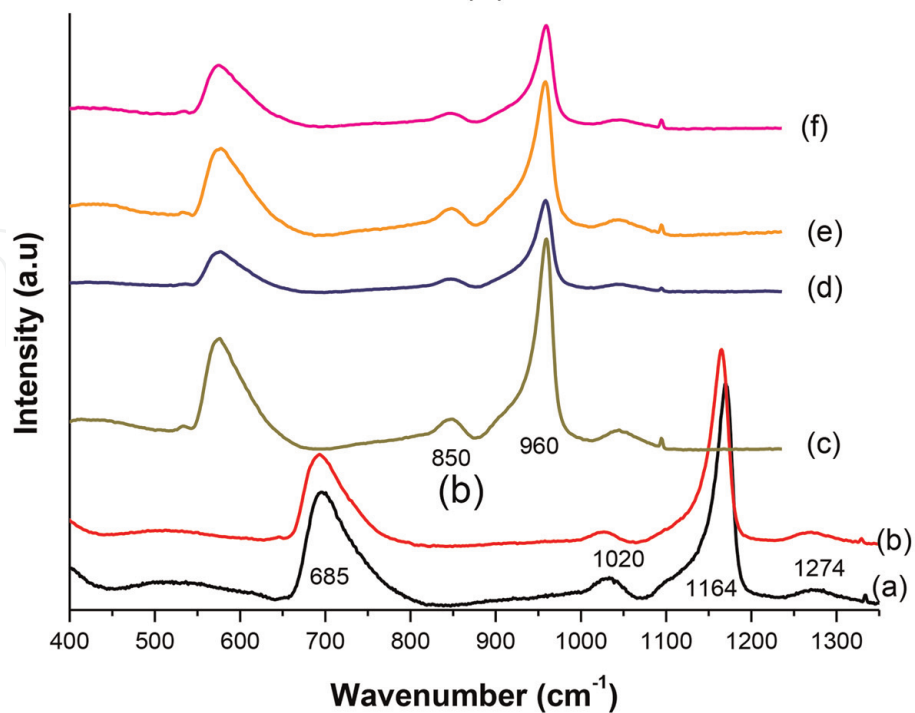
of linked tetrahedral that may be found in crystalline, glassy phosphates and silicate because it can detect the local changes in the environment of Si—O—Si and P—O—P bonds [1, 2].

The Raman spectra were recorded on powder of glasses using a Labram HR800 micro Raman model operating in the 50–4000  $\text{cm}^{-1}$  range at room temperature equipped with an internal He-Ne laser source ( $\lambda = 488 \text{ nm}$ ).

**Figure 2a** reported the Raman spectra of zinc phosphate glasses having a general formula  $(50-x/2)\text{Na}_2\text{O}-x\text{ZnO}-(50-x/2)\text{P}_2\text{O}_5$  ( $0 \leq x \leq 33 \text{ mol\%}$ ) with an O/P ratio varies from 3 to 3.49.



(a)



(b)

**Figure 2.**

*a.* Raman spectra of  $(50-x/2)\text{Na}_2\text{O}-x\text{ZnO}-(50-x/2)\text{P}_2\text{O}_5$  glasses: (a) 0 mol% ZnO, (b) 10 mol% ZnO, (c) 20 mol% ZnO, (d) 25 mol% ZnO, (e) 30 mol% ZnO, (f) 33 mol% ZnO. *b.* Raman spectra of  $(0.9-x)\text{NaPO}_3-x\text{SiO}_2-0.1\text{ZnO}$  ( $0 \leq x \leq 0.1 \text{ mol}$ ) glasses: (a) 0 mol  $\text{SiO}_2$ , (b) 0.02 mol  $\text{SiO}_2$ , (c) 0.04 mol  $\text{SiO}_2$ , (d) 0.06 mol  $\text{SiO}_2$ , (e) 0.08 mol  $\text{SiO}_2$ , (f) 0.10 mol  $\text{SiO}_2$ .

For undoped zinc phosphate glasses, Raman spectrum revealed a large band around  $1274\text{ cm}^{-1}$  and three weaker peaks at 1164, 685, and 380 respectively as shown in **Figure 2a**.

The bands located at 1274 and  $1164\text{ cm}^{-1}$  are assigned to the asymmetric and symmetric vibrations of  $\text{PO}_2$  groups in metaphosphate chains ( $\text{Q}^2$ ) [12, 13, 15, 29, 32, 33]. The large band at about  $685\text{ cm}^{-1}$  is attributed to the symmetric vibration of the bridging oxygen linking two  $\text{PO}_4$  tetrahedrons ( $\text{P—O—P}$ ) in metaphosphate chains [12, 13, 15, 29, 32, 33]. The low frequency attributed to the faint band at  $380\text{ cm}^{-1}$  is related to the bending motion of phosphate polyhedral [12, 13, 15, 29, 32, 33].

With increasing MO content, we observe some decrease of the overall background located at  $600\text{--}800\text{ cm}^{-1}$  and  $1100\text{--}1300\text{ cm}^{-1}$ . These spectral changes can be correlated to the distortion of  $\text{P—O—P}$  band which induces the shortening of the infinite metaphosphate chains suggesting the formation of pyrophosphate groups ( $\text{Q}^1$ ) with the increase of the O/P ratio [12, 13, 15, 29, 32, 33].

From **Figure 2a**, it seems that the intensity of bands located at 1164 and  $685\text{ cm}^{-1}$  decrease when MO oxide is progressively introduced. However, the Raman spectra revealed the displacement of these bands to higher frequencies to 1180 (d, e) and  $780\text{ cm}^{-1}$  (d, e, f) with 30 and 33 mol% of MO level. This result can be probably due to the higher  $\pi$  character of  $\text{P—NBO}$  bands that induces the depolymerization of infinite metaphosphate chains when MO oxide is progressively added.

Similar Raman spectroscopic analysis have been recorded for  $(0.9-x)\text{NaPO}_3\text{-}x\text{SiO}_2\text{-}0.1\text{ZnO}$  ( $0 \leq x \leq 0.1$  mol) glass compositions as shown in **Figure 2b**.

The incorporation of  $\text{SiO}_2$  oxide to the phosphate network generates the appearance of the asymmetric band around  $850\text{ cm}^{-1}$  attributed to  $\text{Si—O—Si}$  bending modes. The band located at  $560\text{ cm}^{-1}$  is attributed to  $\text{Si—O—Si}$  intertetrahedral linkages obtained in calcium and magnesium rich silicate glasses in order to link the distorted metaphosphate groups when  $\text{SiO}_2$  oxide is added [12, 13, 15, 29, 32, 33].

#### 2.4.3 $^{31}\text{P}$ MAS-NMR spectroscopy

The  $^{31}\text{P}$  MAS-NMR spectra of  $(50-x/2)\text{Na}_2\text{O-xZnO-(}50-x/2)\text{P}_2\text{O}_5$  glasses are shown in **Figure 3**.

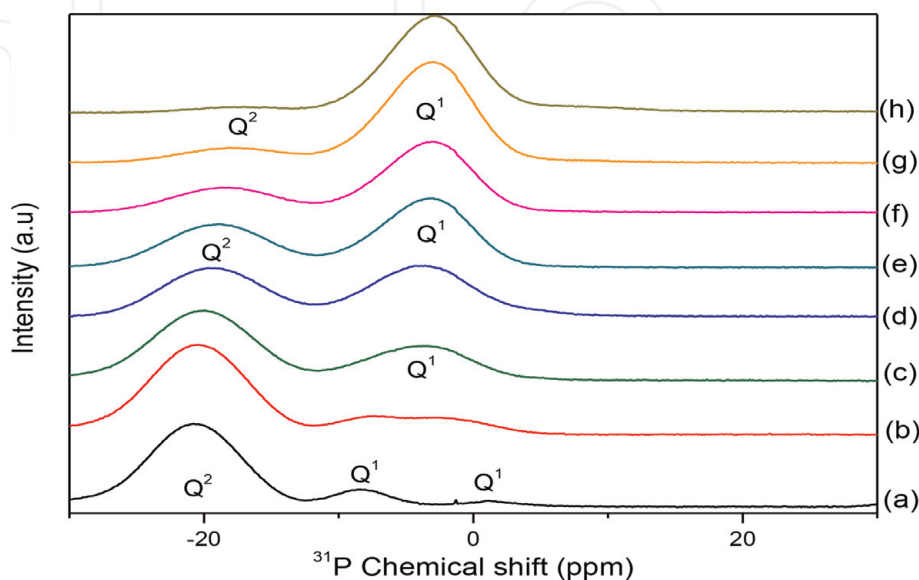


**Figure 3.**  $^{31}\text{P}$  MAS-NMR spectra of  $(50-x/2)\text{Na}_2\text{O-xZnO-(}50-x/2)\text{P}_2\text{O}_5$  glasses: (a) 0 mol% ZnO, (b) 5 mol% ZnO, (c) 10 mol% ZnO, (d) 15 mol% ZnO, (e) 20 mol% ZnO, (f) 25 mol% ZnO, (g) 30 mol% ZnO, (h) 33 mol% ZnO.

The characteristic features of undoped zinc phosphate glasses are isotopic peaks at  $-21$  and  $-6.88$  ppm. The first one is attributed to the  $Q^2$  tetrahedral sites in metaphosphate groups and the second is assigned to the  $Q^1$  groups at the end of chain [12, 13, 15, 29, 32, 33].

Based on literature, the chemical shift at  $+1.4$  ppm is attributed to  $NaPO_3$  chain end groups. From **Figure 3**, one can note the appearance of two isotopic peaks around  $21$ – $18.80$  ppm and  $-6.88$ – $-3.90$  ppm for the glass series.

When the MO oxide is introduced to the vitreous network, the intensity peak attributed to  $Q^1$  tetrahedral sites increases and becomes the major spectral feature [12, 13, 15, 29, 32, 33]. These results are in good agreement for zinc phosphate glasses with the structural study of  $(100-x)NaPO_3-xZnO$  glasses ( $0 \leq x \leq 33.3$  mol %) performed by Montagne et al. [12, 13, 15, 29, 32, 33].

From **Figure 3**, it seems that  $^{31}P$  MAS-NMR spectra exhibit only single peak assigned to  $Q^1$  tetrahedral sites attributed to pyrophosphate groups resulted from the distortion of metaphosphate chains when MO oxide is progressively introduced.

Furthermore, the phosphorus chemical shift depends essentially on the phosphorus-ligand bond (P-O) for phosphate compounds and the electronic density of the non-bridging oxygen (NBO). **Figure 3** mentioned that the  $Q^2$  chemical shift becomes less shielded when MO is added. This decrease is probably due to the higher electronegativity of  $M^{2+}$  compared to  $Na^+$  also the increase of  $\pi$  fraction of P-NBO resulting from the decondensation of phosphate chains when ZnO is incorporated. This suggests that  $Zn^{2+}$  ions are only bonded to pyrophosphate groups described by  $Q^1$  tetrahedral sites. As a result the increase of shielding  $Q^2$  sites from  $-21$  ppm in  $NaPO_3$  glass to  $-18.80$  ppm in  $33.5 Na_2O-33 ZnO-33.5 P_2O_5$  glass composition [12, 13, 15, 29, 32, 33].

#### 2.4.4 UV-VIS spectroscopy

UV-VIS-NIR absorption spectra of the glassy compounds were carried out by means of Perkin-Elmer Lambda 950 spectrometer at room temperature under air. Optical measurements were recorded in the range of 200 and 1800 nm.

Optical absorption, particularly the absorption edge, is useful for the investigation of optically-induced transitions and for getting information about the band gap energy [4, 10, 11, 14, 16, 37, 41]. This parameter is very interesting for the applications of the materials to be studied. It is known that the optical transition occurs through the region between conduction and valence bands (optical band gap) directly or indirectly.

However, the optical transition involves an energy transfer caused by electron transitions between conduction and valence bands [4, 10, 11, 14, 16, 37, 41].

The optical absorption coefficient  $\alpha(h\nu)$  of the prepared glasses was calculated at different wavelengths by using the relation [4, 10, 11, 14, 16, 37, 41]:

$$\alpha = \frac{1}{d} \ln \left( \frac{I}{I_0} \right) \quad (4)$$

where  $d$  represents the thickness of the glass composition and  $\ln \left( \frac{I}{I_0} \right)$  is the absorbance.

For the optical measurements, one can note the absence of the absorption sharp edge which characterizes the vitreous nature of the prepared glasses [4, 10, 11, 14, 16, 37, 41].

According to Davis and Mott, the expression of the absorption coefficient  $\alpha(\nu)$  as a function of photon energy ( $h\nu$ ) for direct and indirect optical absorption, was given by the relation as follows:

$$\alpha(\nu) = \frac{A(h\nu - E_{opt})^n}{h\nu} \quad (5)$$

where

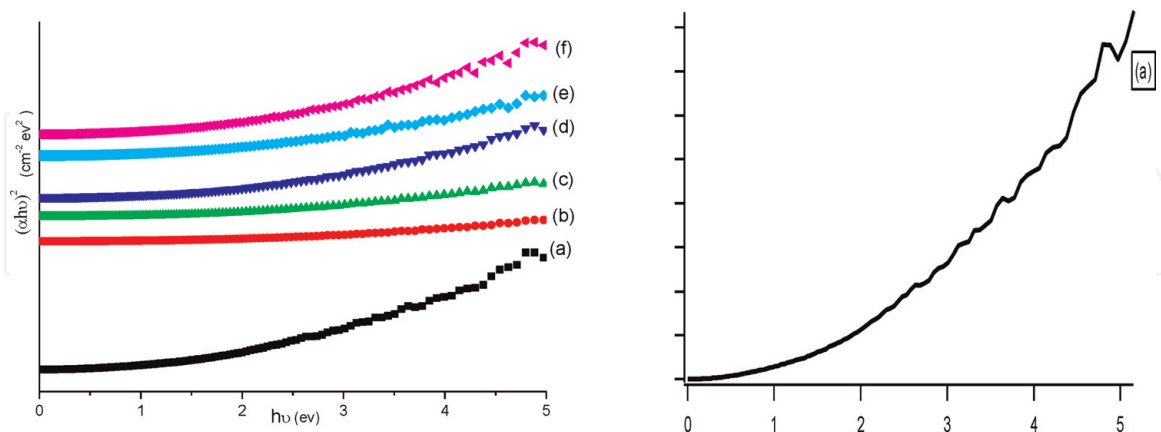
- A: an energy-independent constant
- $E_{opt}$ : the optical band gap energy
- n: a constant which determines the type of the optical transition. For direct allowed transition  $n = 2$  and in the case of indirect allowed transition  $n = \frac{1}{2}$  [4, 10, 11, 14, 16, 37, 41].

For glassy materials, the indirect transitions are valid according to Tauc relations [4, 10, 11, 14, 16, 37, 41].

**Figure 4** represents the variation  $(\alpha h\nu)^2$  versus photon energy ( $h\nu$ ) for  $(0.9-x)\text{NaPO}_3-x\text{SiO}_2-0.1\text{ZnO}$  ( $0 \leq x \leq 0.1$  mol) series glasses.

The values of indirect optical band gap energy ( $E_{opt}$ ) were determined by the extrapolation of the linear region of  $(\alpha h\nu)^2$  against photon energy ( $h\nu$ ) plots at  $(\alpha h\nu)^2 = 0$ . This latter shows that the  $E_{opt}$  increases with the incorporation  $\text{SiO}_2$  from 1.5 to 2.35 eV. This quantity is not only influenced by the chemical composition also by the structural rearrangement in the glass matrix [4, 10, 11, 14, 16, 37, 41]. **Figure 5** shows clearly that the  $E_{opt}$  values dependent strongly on the composition of the glass also on the oxygen bonding in the vitreous network [4, 10, 11, 14, 16, 37, 41]. Any changes of oxygen bonding suggesting the formation of non-bridging oxygen (NBOs) causes a change of the absorption characteristics of the glass [4, 10, 11, 14, 16, 37, 41].

The higher energy is required to excite an electron from bridging oxygen (BO) than from non-bridging oxygen (NBO). As a result the increase in  $E_{opt}$  values [4, 10, 11, 14, 16, 37, 41].



(a) The  $(\alpha h\nu)^2$  as a function of photon energy of  $h\nu$  of  $0.9\text{NaPO}_3-0.1\text{ZnO}$  glass composition  
 \*The  $E_{opt}$  values were determined by the extrapolation of the linear region of  $(\alpha h\nu)^2$  against photon energy ( $h\nu$ ) plots at  $(\alpha h\nu)^2=0$ .

**Figure 4.**  
 The  $(\alpha h\nu)^2$  as a function of photon energy of  $h\nu$  of  $(0.9-x)\text{NaPO}_3-x\text{SiO}_2-0.1\text{ZnO}$  ( $0 \leq x \leq 0.1$  mol) glasses: (a) 0 mol  $\text{SiO}_2$ , (b) 0.02 mol  $\text{SiO}_2$ , (c) 0.04 mol  $\text{SiO}_2$ , (d) 0.06 mol  $\text{SiO}_2$ , (e) 0.08 mol  $\text{SiO}_2$ , (f) 0.10 mol  $\text{SiO}_2$ .  
 \*Obtaining the lines corresponding to the curves of  $(\alpha h\nu)^2$  against photon energy ( $h\nu$ ) is probably due to the superposition effect for all the glass compositions.



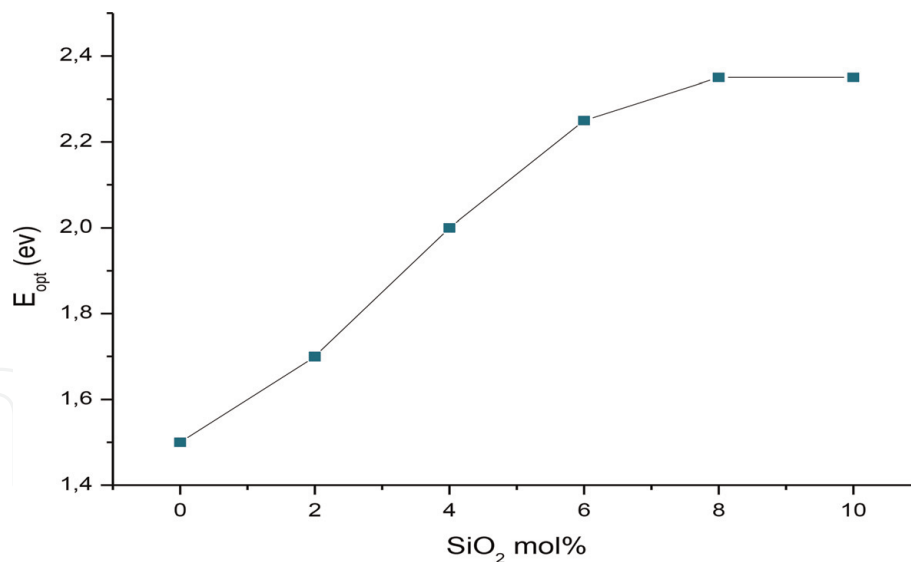


**Figure 5.**

Variation of optical band gap energy of  $(0.9-x)\text{NaPO}_3-x\text{SiO}_2-0.1\text{ZnO}$  ( $0 \leq x \leq 0.1$  mol) glass series.

When  $x$  increases from 0 to 10 mol% of  $\text{SiO}_2$ , the optical band gap energy rises from 1.5 to 2.35 eV. This variation can be explained by the structural modifications which suggest the distortion of metaphosphate chains inducing the increase in the number of non-bridging oxygen (NBOs).

Because the NBOs bonds are predominantly ionic character and consequently have lower bond energies [34]. The higher value of the band gap energy revealed the increase of the cross-linking network due the introduction of  $\text{SiO}_2$  [4, 10, 11, 14, 16, 37, 41].

From **Figure 5**, it seems that the  $E_{\text{opt}}$  is in the order of 2.35 eV for 0.82  $\text{NaPO}_3-0.08$   $\text{SiO}_2-0.1$   $\text{ZnO}$  and 0.8  $\text{NaPO}_3-0.1$   $\text{SiO}_2-0.1$   $\text{ZnO}$  glass compositions. This result can be correlated to the structural changes due to the formation of P-O-Si ionic bands [11].

### 3. Thermochemical study of phosphate glasses

#### 3.1 Calorimetric dissolution of zinc, manganese and magnesium phosphate glasses

The calorimetric study was performed by determining the energy resulting from the dissolution of the glasses in a suitable solvent [11–13, 15, 29, 32, 33, 42].

Phosphate glasses are soluble in mineral acids [11–13, 15, 29, 32, 33, 42]. Furthermore, the dissolution process has been carried out in order to find the suitable solvent which dissolves entirely the glassy compounds and should not give rise to any secondary phenomena.

For this purpose, our investigations were covered all the usual acids, bases and their mixtures such as:  $\text{HNO}_3$ ,  $\text{HCl}$ ,  $\text{NaOH}$ ,  $\text{KOH}$ ,  $\text{CH}_3\text{COOH}$ .

The calorimetric profile shows that the 4.5% weight of phosphoric acid solution is the best solvent for the thermochemical requirements of phosphate glasses.

The dissolution of phosphate glasses were recorded by means the C80 (SETARAM) at 25°C. This equipment possesses two identical cells: the reference and the measuring cell. The reference cell should contain only the solvent but the measuring cell was provided with the solid to be dissolved or the liquid to be mixture. The superior compartment contains the attack solution (solvent) which is tightly separated from the lower one by a movable cover.

The reference and the measuring cell are surrounded by thermoelectric piles with high performance. These latter permit to detect the heat flow resulted from

the dissolution, mixing or dilution process. The integration of the raw signal determined the heat dissolution of the studied compound.

Experiments were carried out by dissolving the same mass of solids (25 mg) in 4.5 ml of solvent.

The plots of heat dissolution of glasses ( $\Delta_{\text{sol}}H$  (kJ mol<sup>-1</sup>)) are shown in **Figure 6**.

For (50-x/2)Na<sub>2</sub>O-xZnO-50-x/2)P<sub>2</sub>O<sub>5</sub> glass composition, it seems that the dissolution phenomenon is endothermic for lower ZnO content and becomes exothermic when ZnO oxide is progressively incorporated in the vitreous network.

Furthermore, the change in thermal signs is probably correlated to structural modifications of metaphosphate groups (Q<sup>2</sup>) suggesting the formation of pyrophosphate units (Q<sup>1</sup>) when ZnO oxide is introduced.

These results were correlated to spectroscopic investigations which revealed the formation of pyrophosphate groups for zinc, manganese and magnesium phosphate glasses, resulting from the cleavage of the P-O-P bridges when the amount of MO oxide is progressively increases [11–13, 15, 29, 32, 33, 42].

### 3.2 Thermochemical study of zinc phosphate glasses

Calorimetric study of glasses has been carried out for several decades. However, the thermochemical investigations of glassy compounds have been considered using a thermodynamic approach based on the Miedema's model in order to evaluate the formation enthalpy of binary alloys [42].

In the case of glassy compounds, the knowledge of the formation enthalpy is an important chemical data which can be used to determine the Gibbs free energy of formation of the selected compounds and to have an idea about their stability.

The determination of the formation enthalpy of (100-x)NaPO<sub>3</sub>-xZnO glass series involves the formation enthalpy of sodium trimetaphosphate, (NaPO<sub>3</sub>)<sub>3</sub>, crystal). Because of the very old value reported in literature [42], this quantity has been determined again by the same technique.

#### 3.2.1 Synthesis and characterization of samples

Sodium trimetaphosphate (NaPO<sub>3</sub>)<sub>3</sub>, was synthesized by thermal decomposition of sodium dihydrogen phosphate (NaH<sub>2</sub>PO<sub>4</sub>). This later was obtained by thermal

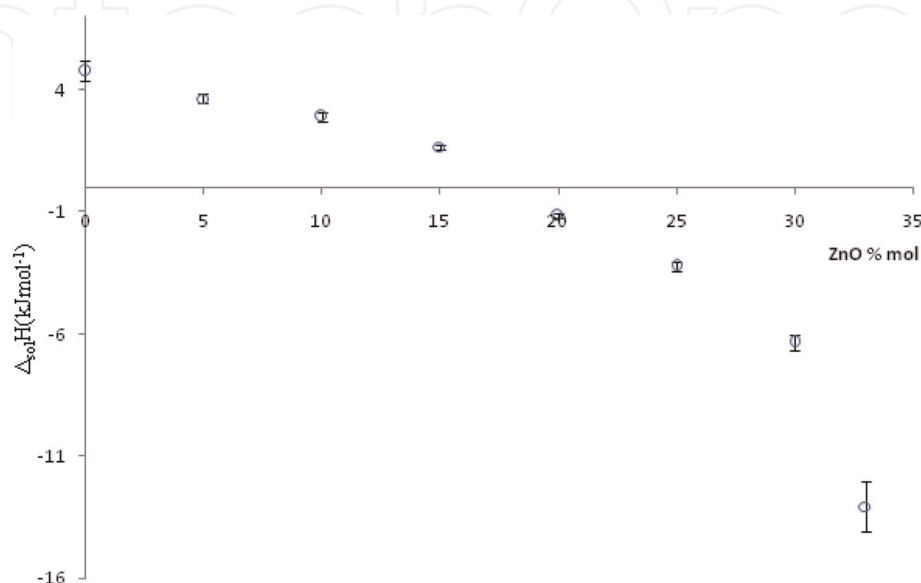


**Figure 6.**  
Evolution of molar enthalpy of dissolution of (100-x)NaPO<sub>3</sub>-xZnO (0 ≤ x ≤ 33 mol%) glasses.

dehydration of its commercial monohydrate from  $\text{NaH}_2\text{PO}_4 \cdot \text{H}_2\text{O}$  (Fluka of purity higher than 99%) at  $150^\circ\text{C}$  during 24 hours.

$\text{NaH}_2\text{PO}_4$  was placed in the furnace, then the temperature increases from  $200$  to  $300^\circ\text{C}$  during 24 hours in order to eliminate residual water and volatile gases. After any heat treatment, the powder was crushed.

Then, the temperature increases and maintains  $500^\circ\text{C}$  for one night. The final product was tested using an X-ray diffraction equipped by SEIFERT-XRD 3000 TT diffractometer which confirms that the final product is the sodium trimetaphosphate.

### 3.3 Cycle for sodium trimetaphosphate ( $(\text{NaPO}_3)_3$ , crystal)

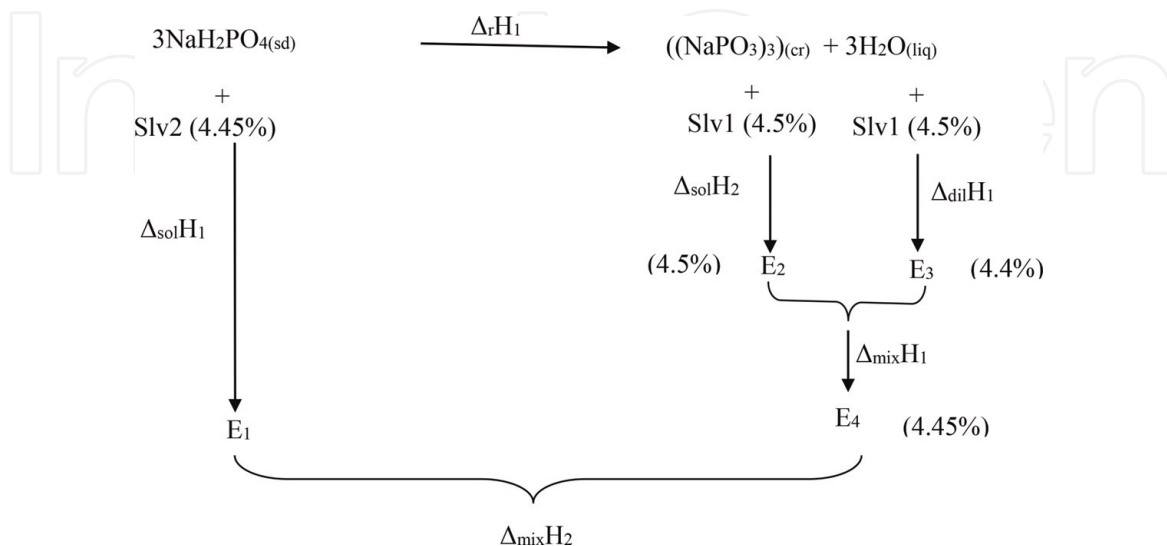
Generally, the direct determination of the formation enthalpy of any compounds is impossible. For this reason, our investigation is based on considering a particular reaction which involves the studied compounds with other reactants and products.

The knowledge of the enthalpy of the hypothetical reaction and the formation enthalpy of the reactants and products allow determining the formation enthalpy of the compound to be studied.

For the sodium trimetaphosphate ( $(\text{NaPO}_3)_3$ , crystal); the following thermochemical cycle has been studied [42]. This later put into consideration the chemical reaction which involves dissolution, dilution and mixing processes.

The designed states from E1 to E4 are the solutions obtained from different chemical operations [42]:

- E1 state presents the phenomena of dissolution for  $\text{NaH}_2\text{PO}_4$  in Slv2 (4.45%) ( $\Delta_{\text{sol}}H_1$ ).
- E2 state designed the dissolution process of  $(\text{NaPO}_3)_3$  in Slv1 (4.5%) ( $\Delta_{\text{sol}}H_2$ ).
- E3 state designed the dilution process of  $3\text{H}_2\text{O}_{(\text{liq})}$  ( $\Delta_{\text{dil}}H_1$ ).
- E4 state designed the mixing process of E2 + E3 states ( $\Delta_{\text{mix}}H_1$ ).



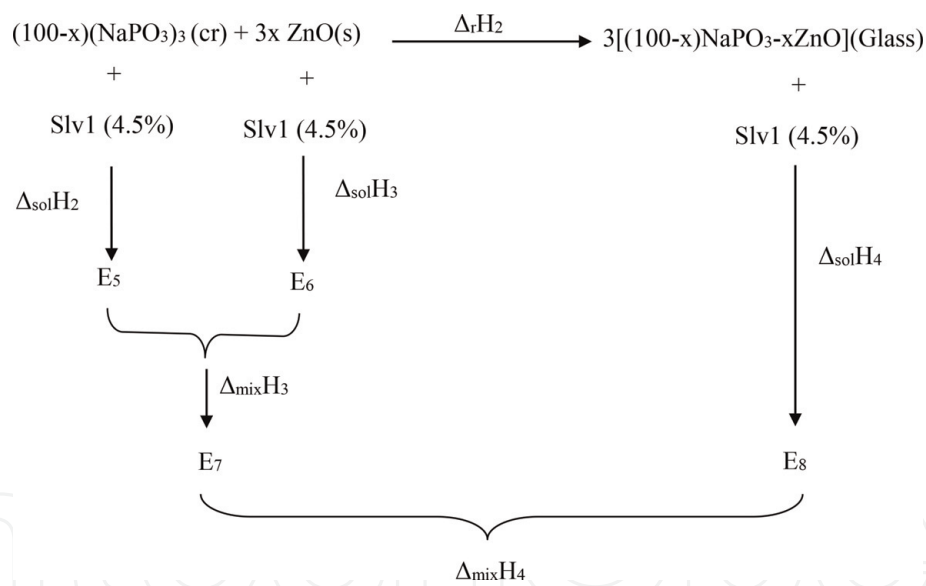
$\Delta_r H_1$  can be expressed as  $\Delta_r H_1 = 3 \Delta_{\text{sol}}H_1 + \Delta_{\text{mix}}H_2 - \Delta_{\text{mix}}H_1 - \Delta_{\text{sol}}H_2 - \Delta_{\text{dil}}H_1$  in which  $\Delta_{\text{sol}}H$  are molar quantities.

So the whole results allow to derive the enthalpy of reaction (R1) at 298.15 K. Taking into account the enthalpies of formation of  $\text{NaH}_2\text{PO}_4$  (s) and  $\text{H}_2\text{O}$  (liq) [42], we can derive that for sodium trimetaphosphate ( $(\text{NaPO}_3)_3$ , (crystal)) at 298.15 K.

### 3.4 Cycle for $\text{Na}_2\text{O-ZnO-P}_2\text{O}_5$ series glass

For zinc-based phosphate glasses, the formation enthalpy of the glass series can be determined by considering a hypothetical reaction based on  $(\text{NaPO}_3)_3$  (crystal) and  $\text{ZnO}$  (sd). Their formation enthalpies can be derived by considering the following cycle which involves dissolution and mixing processes. The designed states from E5 to E8 are the solutions resulted from the different chemical operations [42]:

- E5 state presents the phenomena of dissolution for  $(\text{NaPO}_3)_3$  in Slv1 (4.5%) ( $\Delta_{\text{solH}_2}$ ).
- E6 state designed the dissolution process of  $\text{ZnO}$  in Slv1 (4.5%) ( $\Delta_{\text{solH}_3}$ ).
- E7 state designed the mixing process of E5 + E6 states ( $\Delta_{\text{mixH}_3}$ ).
- E8 state designed the dissolution process of glasses in Slv1 (4.5%) ( $\Delta_{\text{solH}_4}$ ).



According to this cycle  $\Delta_r\text{H}_2$  can be expressed as:  $\Delta_r\text{H}_2 = (100-x) \Delta_{\text{solH}_2} + 3x \Delta_{\text{solH}_3} + \Delta_{\text{mixH}_3} + \Delta_{\text{mixH}_4} - 3\Delta_{\text{solH}_4}$  when E7 and E8 states are identical ( $\Delta_{\text{mixH}_4} \approx 0$ ) [42]. This quantity also equals:

$$\begin{aligned}
 \Delta_r\text{H}_2 = & 3 \Delta_f\text{H} [(100 - x)\text{NaPO}_3 - x\text{ZnO, glass}] \\
 & - (100 - x)\Delta_f\text{H} ((\text{NaPO}_3)_3, \text{crystal}) - 3x \Delta_f\text{H} (\text{ZnO, sd})
 \end{aligned} \tag{6}$$

So, the standard enthalpy of formation of the glass can be derived as:

$$\begin{aligned}
 \Delta_f\text{H}^\circ(\text{glass}) = & 1/3(100 - x)(\Delta_{\text{solH}}(\text{NaPO}_3)_3, \text{crystal}) + \Delta_f\text{H}^\circ(\text{NaPO}_3)_3, \text{cr}) \\
 & + x(\Delta_{\text{solH}}(\text{ZnO, sd}) + \Delta_f\text{H}^\circ(\text{ZnO, sd})) - \Delta_{\text{solH}}(\text{glass}) + 1/3\Delta_{\text{mixH}_3}
 \end{aligned} \tag{7}$$

## 3.4.1 Dissolution processes

**Tables 5–7** show the dissolution heat ( $Q_r$ ) of increasing the moles number ( $n$ ) of  $\text{NaH}_2\text{PO}_4$ ,  $(\text{NaPO}_3)_3$  and  $\text{ZnO}$  solids in their corresponding solvents [42].

**Table 5** presents the dissolution process of  $\text{NaH}_2\text{PO}_4$  with the variation of the quantity ( $n$  (mmol)) to be dissolved in 4.5 ml of phosphoric acid solution (4.45% (w/w)  $\text{H}_3\text{PO}_4$ ) (Slv2).

**Table 6** presents the dissolution process of  $(\text{NaPO}_3)_3$  with the variation of the quantity ( $n$  (mmol)) to be dissolved in 4.5 ml of phosphoric acid solution (4.5% (w/w)  $\text{H}_3\text{PO}_4$ ) (Slv1).

**Table 7** presents the dissolution process for  $\text{ZnO}$  with the variation of the quantity ( $n$  (mmol)) to be dissolved in 4.5 ml of phosphoric acid solution (4.5% (w/w)  $\text{H}_3\text{PO}_4$ ) (Slv1).

The plots of the variation of the measuring heats as a function of the moles number of solid leads to straight lines whose expressed as:  $Q_r = An+b$ .

The slope ( $A$ ) presents the molar dissolution enthalpy ( $\Delta_{\text{sol}}H$ ) and  $b$  is the intercept increment.

Referring to a mathematical treatment developed in literature, the increment  $b$  is statistically not significant which leads to derive the dissolution enthalpy as [42]:

$\text{NaH}_2\text{PO}_4$ (sd) in Slv2 ( $\Delta_{\text{sol}}H_1$ )		
$n$ (mmol)	$Q_r$ (J)	$uQ_r$ (J)
0.2548	1.084	0.05
0.3700	1.328	0.08
0.3440	1.282	0.06
0.3000	1.167	0.11
0.1366	0.680	0.06

$Q_r$ : Heat of solution.

Slv2: 4.45% (w/w)  $\text{H}_3\text{PO}_4$ .

<sup>a</sup>Standard uncertainties  $u$  are  $u(T) = 0.01$  K,  $u(p) = 10$  kPa.

**Table 5.**

Enthalpy of solution of  $\text{NaH}_2\text{PO}_4$  (sd) in 4.45% (w/w)  $\text{H}_3\text{PO}_4$  at the temperature  $T = 298.15$  K and pressure  $p = 0.1$  MPa (level of confidence = 0.68).<sup>a</sup>

$(\text{NaPO}_3)_3$ (cr) in Slv1 ( $\Delta_{\text{sol}}H_2$ )		
$n$ (mmol)	$Q_r$ (J)	$uQ_r$ (J)
0.1995	0.950	0.08
0.2473	1.171	0.06
0.2990	1.370	0.07
0.3452	1.590	0.12
0.2626	1.240	0.10

$Q_r$ : Heat of solution.

Slv1: 4.5% (w/w)  $\text{H}_3\text{PO}_4$ .

<sup>a</sup>Standard uncertainties  $u$  are  $u(T) = 0.01$  K,  $u(p) = 10$  kPa.

**Table 6.**

Heat of solution of  $(\text{NaPO}_3)_3$ (cr) in 4.5% (w/w)  $\text{H}_3\text{PO}_4$  at the temperature  $T = 298.15$  K and  $p = 0.1$  MPa (level of confidence = 0.68).<sup>a</sup>

ZnO (sd) in Slv1 ( $\Delta_{\text{sol}}\text{H}_3$ )		
n (mmol)	$Q_r$ (J)	$u(Q_r)$ (J)
0.2736	-26.081	0.12
0.3625	-34.600	0.33
0.2461	-23.500	0.24
0.2211	-21.215	0.22
0.3060	-29.124	0.50
0.3350	-32.010	0.21

$Q_r$ : Heat of solution.  
 Slv1: 4.5% (w/w)  $\text{H}_3\text{PO}_4$ .  
<sup>a</sup>Standard uncertainties  $u$  are  $u(T) = 0.01 \text{ K}$ ,  $u(p) = 10 \text{ kPa}$ .

**Table 7.**  
 Enthalpy of solution of ZnO (sd) in 4.5% (w/w)  $\text{H}_3\text{PO}_4$  at  $T = 298.15 \text{ K}$  and  $p = 0.1 \text{ MPa}$  (level of confidence = 0.68).<sup>a</sup>

$$\Delta_{\text{sol}}\text{H} = \frac{\sum(w_i * \Delta\text{H}_i n_i)}{\sum(w_i * n_i^2)} = A \text{ (kJmol}^{-1}\text{)}$$

where ( $w_i$ ) is the reciprocal of the variance on  $\Delta\text{H}_i$  ( $w_i = 1/\sigma^2 \Delta\text{H}_i$ ), and  $\Delta\text{H}_i$  is the energy resulting by dissolving  $n_i$  (mol) of the corresponding product in the phosphoric acid solution.

Equations of the lines are as follows [42]:

$$\Delta_{\text{sol}}\text{H}_1 = 4.01 n \quad (8)$$

for ( $\text{NaH}_2\text{PO}_4$ ) (sd) in 4.45% weight of  $\text{H}_3\text{PO}_4$  solution.

$$\Delta_{\text{sol}}\text{H}_2 = 4.66 n \quad (9)$$

for ( $(\text{NaPO}_3)_3$ , (crystal)) in 4.5% weight of  $\text{H}_3\text{PO}_4$  solution.

For ZnO (sd) in 4.5% weight of  $\text{H}_3\text{PO}_4$  solution.

$$\Delta_{\text{sol}}\text{H}_3 = -95.50 n \quad (10)$$

**Table 8** gathers the values of molar dissolution enthalpies with the corresponding errors.

For zinc phosphate glasses, experiments were carried out by dissolving the same mass of solids (25 mg) in 4.5 ml of 4.5% weight of  $\text{H}_3\text{PO}_4$  solution [42].

Compound	$\text{NaH}_2\text{PO}_4$ (sd) in Slv2	$(\text{NaPO}_3)_3$ (sd) in Slv1	ZnO (sd) in Slv1
$\Delta_{\text{sol}}\text{H}$ (kJ/mol)	$\Delta_{\text{sol}}\text{H}_1 = 4.01 \pm 0.47$	$\Delta_{\text{sol}}\text{H}_2 = 4.66 \pm 0.44$	$\Delta_{\text{sol}}\text{H}_3 = -95.5 \pm 2.7$

Slv1: 4.5% (w/w)  $\text{H}_3\text{PO}_4$ .  
 Slv2: 4.45% (w/w)  $\text{H}_3\text{PO}_4$ .  
<sup>a</sup>Standard uncertainties  $u$  are  $u(T) = 0.01 \text{ K}$ ,  $u(p) = 10 \text{ kPa}$ .

**Table 8.**  
 Molar enthalpy of solution of dissolved compounds at the temperature  $T = 298.15 \text{ K}$  and pressure  $p = 0.1 \text{ MPa}$  (level of confidence = 0.68).<sup>a</sup>

Composition	$\Delta_{\text{sol}}\text{H}$ (kJ/mol)	$u$ ( $\Delta_{\text{sol}}\text{H}$ ) (kJ/mol)
NaPO <sub>3</sub>	4.80	0.45
95 NaPO <sub>3</sub> -5 ZnO	3.70	0.20
90 NaPO <sub>3</sub> -10 ZnO	2.92	0.15
85 NaPO <sub>3</sub> -15 ZnO	1.70	0.10
80 NaPO <sub>3</sub> -20 ZnO	-1.15	0.10
75 NaPO <sub>3</sub> -25 ZnO	-3.21	0.20
70 NaPO <sub>3</sub> -30 ZnO	-6.34	0.32
67 NaPO <sub>3</sub> -33 ZnO	-13.05	1.00

<sup>a</sup>Standard uncertainties  $u$  are  $u(T) = 0.01$  K,  $u(p) = 10$  kPa.

**Table 9.**

Evolution of heat solution of  $(100-x)\text{NaPO}_3\text{-}x\text{ZnO}$  phosphate glasses in 4.5% (w/w)  $\text{H}_3\text{PO}_4$  at the temperature  $T = 298.15$  K and pressure  $p = 0.1$  MPa (level of confidence = 0.68).<sup>a</sup>

**Table 9** reports the variation of the heat dissolution for the glass series published in a previous work [33]. This evolution shows that the dissolution heat decreases linearly with the incorporation of ZnO oxide. As a result the inversion in the thermal signs for the studies glasses. This variation can be explained by the structural changes of the phosphate network suggesting the distortion of metaphosphate chains revealed by <sup>31</sup>P MAS-NMR analysis.

Plotting of dissolution heat versus ZnO proportion ( $\Delta_{\text{sol}}\text{H}$  (kJ mol<sup>-1</sup>)) is reported in **Figure 6**. It seems that the calorimetric dissolution of the glass series is endothermic for lower ZnO proportion and becomes exothermic above 18 mol% of ZnO. This variation can be correlated to the cleavage of P—O—P bridges which suggests the appearance of pyrophosphate groups (Q<sup>1</sup>), revealed by <sup>31</sup>P MAS-NMR spectroscopic analysis, when ZnO oxide is progressively incorporated in the vitreous network [33].

### 3.4.2 Mixing processes

#### 3.4.2.1 For $(\text{NaPO}_3)_3$ crystal cycle

E2 was provided with various amounts of  $(\text{NaPO}_3)_3$  (6–9 mg) which have been dissolved in 4.5% (w/w)  $\text{H}_3\text{PO}_4$  solution but E3 is 4.4% (w/w)  $\text{H}_3\text{PO}_4$  solution. Mixing the same volumes of E2 and E3 (around 2 ml) leads to a solution having the mean value of acid composition (E4 with 4.45% (w/w)  $\text{H}_3\text{PO}_4$  or  $[\text{H}_3\text{PO}_4, 116.90\text{H}_2\text{O}]$ ). Consequently, the concentration of Slv2 was fixed as 4.45% (w/w)  $\text{H}_3\text{PO}_4$  in order to get identical E1 and E4 states. **Table 10** reports E2 + E3 mixing enthalpy for different mole number (n) of  $(\text{NaPO}_3)_3$  added in E2. This allowed to express  $\Delta_{\text{mix}}\text{H}_1$  as:  $\Delta_{\text{mix}}\text{H}_1 = 0.07 n$  ( $R^2 = 0.995$ ) leading to a value of 0.07 kJ per  $(\text{NaPO}_3)_3$  mole [42].

(E<sub>1</sub> + E<sub>4</sub>) mixing process, which noted as ( $\Delta_{\text{mix}}\text{H}_2$ ), was considered in order to check whether or not they correspond to the same final state. This operation led to an undetectable thermal effect [42].

#### 3.4.2.2 For $\text{Na}_2\text{O-ZnO-P}_2\text{O}_5$ glasses cycle

Mixing the same volumes (around 2 ml) of E<sub>5</sub> and E<sub>6</sub> which have the same concentration of phosphoric acid (4.5% (w/w)  $\text{H}_3\text{PO}_4$ ), led to E<sub>7</sub> solution. Were previously added to while The E<sub>5</sub> state was obtained by dissolving the average mass of  $(\text{NaPO}_3)_3$ , (crystal) (27.3 mg) whereas the E<sub>6</sub> state was considered by dissolving

n (mmol)	Q <sub>r</sub> (J)	u(Q <sub>r</sub> ) (J)
0.0187	0.0005	0
0.0257	0.0010	0
0.0157	0.0003	0
0.0300	0.0013	0

<sup>a</sup>Standard uncertainties *u* are  $u(T) = 0.01\text{ K}$ ,  $u(p) = 10\text{ kPa}$ .  
 E2: Solution with various amounts of  $(\text{NaPO}_3)_3$  in 4.5% (w/w)  $\text{H}_3\text{PO}_4$ .  
 E3: 4.4% (w/w)  $\text{H}_3\text{PO}_4$ .  
 Q<sub>r</sub>: Heat of mixing.

**Table 10.**  
 Enthalpy of mixing:  $\Delta_{\text{mix}}H_1$  (E2 + E3) at the temperature  $T = 298.15\text{ K}$  and pressure  $p = 0.1\text{ MPa}$  (level of confidence = 0.68).<sup>a</sup>

Composition	$\Delta_{\text{mix}}H_3$ (E5 + E6) (kJ/ZnO mole)	$u(\Delta_{\text{mix}}H_3)$ (kJ/mol)	$\Delta_{\text{mix}}H_4$ (E7 + E8) (kJ/mol)
95 NaPO <sub>3</sub> -5 ZnO	10.15	0.10	≈0
90 NaPO <sub>3</sub> -10 ZnO	4.00	0.13	≈0
85 NaPO <sub>3</sub> -15 ZnO	5.10	0.21	≈0
80 NaPO <sub>3</sub> -20 ZnO	3.23	0.24	≈0
75 NaPO <sub>3</sub> -25 ZnO	2.74	0.25	≈0
70 NaPO <sub>3</sub> -30 ZnO	3.00	0.15	≈0
67 NaPO <sub>3</sub> -33 ZnO	2.12	0.20	≈0

<sup>a</sup>Standard uncertainties *u* are  $u(T) = 0.01\text{ K}$ ,  $u(p) = 10\text{ kPa}$ .  
 E5: solution with 27.3 mg of  $(\text{NaPO}_3)_3$  in 4.5% (w/w)  $\text{H}_3\text{PO}_4$ .  
 E6: solution with various amounts of ZnO in 4.5% (w/w)  $\text{H}_3\text{PO}_4$ .  
 E8: solution with 25 mg of glass composition in 4.5% (w/w)  $\text{H}_3\text{PO}_4$ .

**Table 11.**  
 Enthalpy of mixing:  $\Delta_{\text{mix}}H_3$  and  $\Delta_{\text{mix}}H_4$  at  $T = 298.15\text{ K}$  and  $p = 0.1\text{ MPa}$  (level of confidence = 0.68).<sup>a</sup>

the various amounts of ZnO so the variation of energy (**Table 11**) is due to the presence of ZnO in the solution. The mixture of E<sub>7</sub> and E<sub>8</sub> states has no detectable thermal effect [42].

### 3.4.3 Dilution processes

For the cycle corresponding to the sodium trimetaphosphate, addition of water to Slv1 [ $\text{H}_3\text{PO}_4 \cdot 115.54\text{ H}_2\text{O}$ ] corresponds to a dilution process. The corresponding energy was calculated by linear interpolation of literature data considering the interval to which belongs each enthalpies of solution of the initial (4.5% (w/w)  $\text{H}_3\text{PO}_4$ ) and final states (4.4% (w/w)  $\text{H}_3\text{PO}_4$ ) [42].

The formation and dilution enthalpies were calculated from Ref. [42] and listed below:

$$\Delta_f H^\circ ([\text{H}_3\text{PO}_4 \cdot 115.54\text{H}_2\text{O}]) = -1288.255 (\text{H}_3\text{PO}_4\ 4.5\%) \quad (11)$$

$$\Delta_f H^\circ ([\text{H}_3\text{PO}_4 \cdot 118.54\text{H}_2\text{O}]) = -1288.272 (\text{H}_3\text{PO}_4\ 4.4\%) \quad (12)$$

Calculation gives  $\Delta_{\text{dil}}H_1 = -0.017\text{ kJ mol}^{-1}\text{ H}_3\text{PO}_4$ .

The formation enthalpy of sodium trimetaphosphate ( $(\text{NaPO}_3)_3$ , crystal) has been deduced as  $(-3762.5 \pm 175)\text{ kJ mol}^{-1}$ . The obtained value differs from the



Composition	$\Delta_f H^\circ$ (kJ/mol)	$u(\Delta_f H^\circ)$ (kJ/mol)
NaPO <sub>3</sub>	-1260	50
95 NaPO <sub>3</sub> -5 ZnO	-1213	49
90 NaPO <sub>3</sub> -10 ZnO	-1174	47
85 NaPO <sub>3</sub> -15 ZnO	-1132	45
80 NaPO <sub>3</sub> -20 ZnO	-1090	44
75 NaPO <sub>3</sub> -25 ZnO	-1070	43
70 NaPO <sub>3</sub> -30 ZnO	-1003	40
67 NaPO <sub>3</sub> -33 ZnO	-973	39

<sup>a</sup>Standard uncertainties  $u$  are  $u(T) = 0.01\text{ K}$ ,  $u(p) = 10\text{ kPa}$ .

**Table 12.**

Formation enthalpy of:  $(100-x)\text{NaPO}_3-x\text{ZnO}$  glasses at the temperature  $T = 298.15\text{ K}$  and pressure  $p = 0.1\text{ MPa}$  (level of confidence = 0.68).<sup>a</sup>

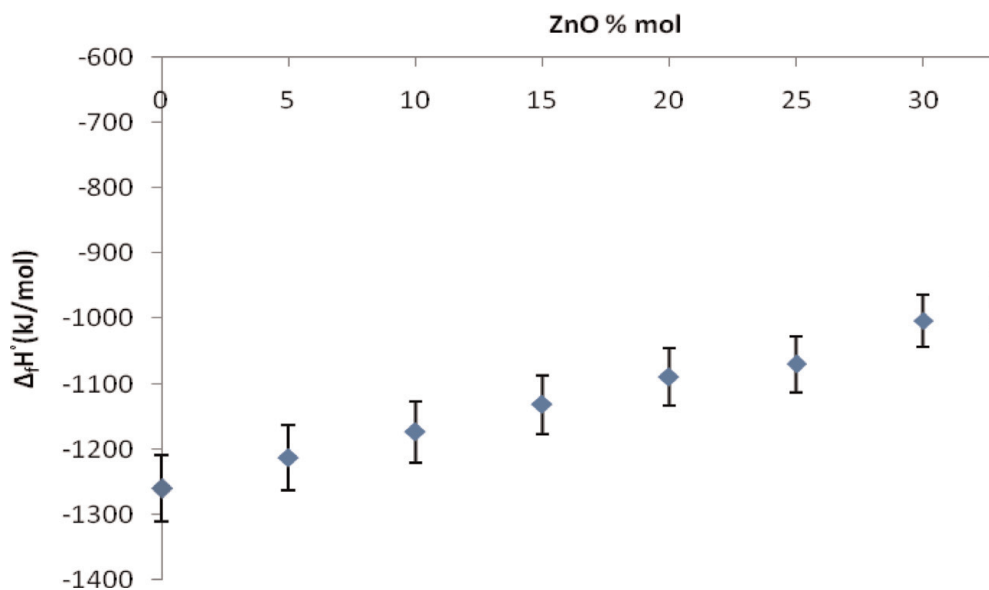


**Figure 7.**

Evolution of the standard enthalpy of formation at standard temperature and pressure of  $(100-x)\text{NaPO}_3-x\text{ZnO}$  ( $0 \leq x \leq 33\text{ mol\%}$ ) glasses [45].

older by only 2.4%. It seems that the calculated value of the formation enthalpy of sodium trimetaphosphate ( $(\text{NaPO}_3)_3$ , crystal) is in good agreement with this determined previously in 1968. This confirms that the synthesized product is probably the sodium trimetaphosphate and not a mixture.

The variation of the formation enthalpy of the glass series are mentioned in **Table 12**. This latter shows that this quantity increases with the addition of ZnO oxide as reported in **Figure 7** [42].

#### 4. Conclusions

The influence of ZnO, MgO, MnO and SiO<sub>2</sub> addition on the structure, physical and optical properties of phosphate glasses and phosphate-based silicate glasses having a general formula:  $(50-x/2)\text{Na}_2\text{O}-x\text{MO}-(50-x/2)\text{P}_2\text{O}_5$  ( $M = \text{Zn, Mn, Mg}$ ) where  $3 \leq \text{O/P} \leq 3.49$ ;  $(50-x)\text{Na}_2\text{O}-x\text{MO}-50\text{P}_2\text{O}_5$  ( $M = \text{Zn, Mn}$ ) with  $\text{O/P} = 3$  ( $0 \leq x \leq 33\text{ mol\%}$ ) and  $(0.9-x)\text{NaPO}_3-x\text{SiO}_2-0.1\text{ZnO}$  ( $0 \leq x \leq 0.1\text{ mol}$ ).

Amorphous state was investigated by means of FTIR, Raman, MAS-NMR and UV-visible spectroscopy in order to study the structural role of MO oxide.

Spectroscopic analysis revealed the formation of pyrophosphate groups ( $Q^1$ ) resulting from the depolymerization of infinite metaphosphate groups ( $Q^2$ ) when the modifying oxide is gradually incorporated.

Furthermore, the indirect optical band gap energy for zinc phosphate-based silicate glasses increases with the addition of  $SiO_2$  oxide. This suggests the increase in the NBOs resulting from the modification of  $P-O-P$  bridges which revealed the shortening of the metaphosphate chains.

On the other hand, the dissolution process is endothermic at lower MO content and become exothermic when MO oxide is progressively incorporated. The change in thermal sign could be correlated to the structural modification inducing the formation of  $P-O-M$  ionic bond which increases the rigidity and the compacity of the vitreous network.

Furthermore, the glass formation enthalpy of  $(100-x)NaPO_3-xZnO$  ( $0 \leq x \leq 33$  mol%) glass series were determine by considering a thermochemical cycle involving the formation enthalpy of sodium trimetaphosphate ( $(NaPO_3)_3$ , crystal). This later was checked in this work.

The glass formation enthalpy increases when ZnO oxide is progressively incorporated in the vitreous network.

When replacing of P by Zn induced a decrease in the binding energy which suggest the increase of the formation enthalpy of the glass series.

Furthermore, the variation of  $T_g$  values reflects an increase of the rigidity of the glass network due to the formation of  $P-O-Zn$  ionic bonds. As a result, the increase in the stability of the phosphate network which is tightly related to the Gibbs free energy of formation  $\Delta_r G^\circ$ .

Because of the large disorder that exists in the vitreous structure, the entropy factor ( $\Delta_r S^\circ$ ) should prevail and induce the decrease in  $\Delta_r G^\circ$  value when ZnO concentration increases.

## Author details


Refka Oueslati Omrani<sup>1\*</sup>, Mohamed Jemal<sup>2</sup>, Ismail Khattech<sup>2</sup>  
and Ahmed Hichem Hamzaoui<sup>1</sup>

<sup>1</sup> Useful Materials Valorization Laboratory, National Center For Research in Materials Sciences, Technological Park of Borj Cedria, Soliman, Tunisia

<sup>2</sup> Université de Tunis El Manar, Faculty of Science, Chemistry Department, Laboratory of Materials Crystal and Applied Thermodynamics LR15SE01, Tunis, Tunisia

\*Address all correspondence to: [refkaoueslati@gmail.com](mailto:refkaoueslati@gmail.com)

## IntechOpen

© 2019 The Author(s). Licensee IntechOpen. This chapter is distributed under the terms of the Creative Commons Attribution License (<http://creativecommons.org/licenses/by/3.0>), which permits unrestricted use, distribution, and reproduction in any medium, provided the original work is properly cited. 

## References

- [1] Sreedhar VB, Basavapoornima CH, Jayasankar CK. Spectroscopic and fluorescence properties properties of  $\text{Sm}^{3+}$  doped zincfluorophosphate glasses. *Journal of Rare Earths*. 2014;**32**: 918
- [2] Aguiar H, Solla EL, Serra J, Conzalez P, Leon B, Malz F, et al. Jager, Raman and NMR study of bioactive  $\text{Na}_2\text{O}$ - $\text{MgO}$ - $\text{CaO}$ - $\text{P}_2\text{O}_5$ - $\text{SiO}_2$  glasses. *Journal of Non-Crystalline Solids*. 2008; **354**:5004-5008
- [3] Zid MHM, Matori KA, Hj S, Aziz A, Zakaria A. Effect of ZnO on the physical and optical band gap of soda lime silicate glass. *International Journal of Molecular Sciences*. 2012;**13**: 7550-7558
- [4] Ibrahim AM, Bader AM, Elshaikh HA, Mostafa AG, Elbashar YH. Effect of CuO addition on the dielectric parameters of sodium zinc phosphate glasses. *Silicon*. 2017. pp. 1265-1274
- [5] Vedeanu N, Stanescu R, Filip S, Ardelean I, Cozar O. IR and ESR investigations on  $\text{V}_2\text{O}_5$ - $\text{P}_2\text{O}_5$ - $\text{BaO}$  glass system with opto-electronic potential. *Journal of Non-Crystalline Solids*. 2012; **358**:1881-1885
- [6] Ahmina W, El Moudane M, Zriouil M, Taibi M. Effect of the content of MnO on the electric-dielectric properties of potassium-phosphate glasses. *Journal of Materials and Environmental Science*. 2017;**11**: 4193-4198
- [7] Waclawska I, Szumera M, Sulowska J. Structural characterization of zinc-modified glasses from the  $\text{SiO}_2$ - $\text{K}_2\text{O}$ - $\text{CaO}$ - $\text{MgO}$ . *Journal of Alloys and Compounds*. 2016;**666**:352-358
- [8] Pascuta P, Bosca M, Borodi G, Vida-Simiti I, Culea E. Thermal, structural and magnetic properties of some zinc phosphate glasses doped with manganese ions. *Journal of Alloys and Compounds*. 2011;**509**:4314-4319
- [9] Oui MA, Azooz MA, Elbatal HA. Optical and infrared spectral investigations of cadmium zinc phosphate glasses doped with  $\text{WO}_3$  or  $\text{MoO}_3$  before and after subjecting to gamma irradiation. *Journal of Non-Crystalline Solids*. 2018;**494**:31-39
- [10] Khor SF, Talib A, Mat Yunus WM. Optical properties of ternary zinc magnesium phosphate glasses. *Ceramics International*. 2012;**38**:935-940
- [11] Omrani RO, Hamzaoui AH, Chtourou R, M'nif A. Structural, thermal and optical properties of phosphate glasses doped with  $\text{SiO}_2$ . *Journal of Non-Crystalline Solids*. 2018; **481**:10-16
- [12] Cherbib MA, Khattech I, Montagne L, Reval B, Jemal M. Structure properties relationship in calcium sodium metaphosphate and polyphosphate glasses. *Journal of Non-Crystalline Solids*. 2018;**485**:1-13
- [13] Oueslati-Omrani R, Kaoutar A, El Jazouli A, Krimi S, Khattech I, Jemal M, et al. Structural and thermochemical properties of sodium magnesium phosphate glasses. *Journal of Alloys and Compounds*. 2015;**632**:766-771
- [14] El-Maaref AA, Badr S, ElOkr KS, Abdel Wahab EA, ElOkr MM. Optical properties and radiatives rates of  $\text{Nd}^{3+}$  doped zinc-sodium phosphate glasses. *Journal of Rare Earths*. 2019;**37**:253-259
- [15] Cherbib MA, Krimi S, El Jazouli A, Khattech I, Montagne L, Reval B, et al. Structure and thermochemical study of strontium sodium phosphate glasses. *Journal of Non-Crystalline Solids*. 2016; **447**:59-65

- [16] Magdas DA, Stefan R, Toloman D, Vedeanu NS. Copper ions influence on lead-phosphate glass network. *Journal of Molecular Structure*. 2014;**1056-1057**: 314-318
- [17] Vedeanu N, Magdas DA, Stefan R. Structural modifications induced by addition of copper oxide to lead-phosphate glasses. *Journal of Non-Crystalline Solids*. 2012;**358**: 3170-3174
- [18] Zhang L, Liu S. Structure and crystallization behavior of  $50\text{CuO}-x\text{TiO}_2-(50-x)\text{P}_2\text{O}_5$ . *Journal of Non-Crystalline Solids*. 2017;**473**:108-113
- [19] Brow RK. Review: The structure simple of phosphate glasses. *Journal of Non-Crystalline Solids*. 2000;**263-264**: 1-28
- [20] Aguiar H, Solla JM, Serra J, Gonzalez P, Leon B, Almeida N, et al. Orthophosphate nanostructures in  $\text{SiO}_2\text{-P}_2\text{O}_5\text{-CaO-Na}_2\text{O-MgO}$  biactive glasses. *Journal of Non-Crystalline Solids*. 2008; **354**:4075-4080
- [21] Abd el Ghany HA. Physical and optical characterization of manganese ions in sodium-zinc-phosphate glass matrix. *IARJSET*. 2018. p. 5
- [22] Khor SF, Talib ZA, Malek F, Cheng EM. Optical properties of ultraphosphate glasses containing mixed divalent zinc and magnesium ions. *Optical Materials*. 2013;**35**:629-633
- [23] Walter G, Vogel J, Hoppe U, Hartmann P. The structure of  $\text{CaO-Na}_2\text{O-MgO-P}_2\text{O}_5$  invert glass. *Journal of Non-Crystalline Solids*. 2001;**296**: 212-223
- [24] Li HC, Wang DG, Hu JH, Chen CZ. Influence of fluoride additions on biological and mechanical properties of  $\text{Na}_2\text{O-CaO-SiO}_2\text{-P}_2\text{O}_5$  glass-ceramics. *Materials Letters*. 2013;**106**:373-376
- [25] Pascuta P, Borodi G, Jumate N, Vida-Simiti I, Viorel D, Culea E. The structural role of manganese ions in some zinc phosphate glasses and glass ceramics. *Journal of Alloys and Compounds*. 2010;**504**:479-483
- [26] Pop L, Bolundut L, Pascuta P, Culea E. Influence of  $\text{Er}^{3+}$  ions addition on thermal and optical properties of phosphate-germanate system. *Journal of Thermal Analysis and Calorimetry*. 2019
- [27] Jlassi I, Elhouichet H, Ferid M. Electrical conductivity and dielectric properties of MgO doped lithium phosphate glasses. *Journal of Physics E*. 2016;**81**:219-223
- [28] Ciceo-Lucacel R, Todea M, Simon V. Effect of selenium addition on network connectivity in  $\text{P}_2\text{O}_5\text{-CaO-MgO-Na}_2\text{O}$  glasses. *Journal of Non-Crystalline Solids*. 2018;**480**:10-13
- [29] Cherbib MA, Khattech I, Montagne L, Reval B, Jemal M. Effect of SrO content on the structure and properties of sodium-strontium metaphosphate glasses. *The Journal of Physical Chemistry A*. 2017:62-68
- [30] Sevastiajova I, Aseev V, Tuzova L, Fedorov Y, Nikonorov N. Spectral and luminescence properties of manganese ions in vitreous lead metaphosphate. *Journal of Luminescence*. 2019:495-499
- [31] Ciceo-Lucacel R, Todea M, Simon V. Effect of selenium addition on network connectivity in  $\text{P}_2\text{O}_5\text{-CaO-MgO-Na}_2\text{O}$  glasses. *Journal of Non-Crystalline Solids*. 2018;**488**:10-13
- [32] Oueslati-Omrani R, Krimi S, Videau JJ, Khattech I, El Jazouli A, Jemal M. Structural investigations and calorimetric dissolution of manganese phosphate glasses. *Journal of Crystalline Solids*. 2014;**389**:66-71
- [33] Oueslati-Omrani R, Krimi S, Videau JJ, Khattech I, El Jazouli A,

- Jemal M. Structural and thermochemical study of Na<sub>2</sub>O-ZnO-P<sub>2</sub>O<sub>5</sub> glasses. *Journal of Crystalline Solids*. 2014;**390**: 5-12
- [34] Hurt JC, Phillips JC. Structural role of zinc oxide in glasses in the system Na<sub>2</sub>O-ZnO-SiO<sub>2</sub>. *Journal of the American Ceramic Society*. 1967;**53**
- [35] Wan MH, Wong PS, Hussin R, Lintang HO, Edud S. Structural and luminescence properties of Mn<sup>2+</sup> ions doped calcium zinc borophosphate glasses. *Journal of Alloys and Compounds*. 2014;**595**:39-45
- [36] Hassaan MY, Moustafa MG, Osouda K, Kubuki S, Nishiba T. 57Fe and 119Sn Mössbauer, XRD, FTIR and DC conductivity study of Li<sub>2</sub>O-Fe<sub>2</sub>O<sub>3</sub>-SnO<sub>2</sub>-P<sub>2</sub>O<sub>5</sub> glass and glass ceramics. *Journal of Alloys and Compounds*. 2018; **765**:121-127
- [37] Mohan S, Kaur S, Kaur P, Singh DP. Spectroscopic investigations of Sm<sup>3+</sup> doped lead alumino-borate glasses containing zinc, lithium and barium oxides. *Journal of Alloys and Compounds*. 2018;**763**:486-495
- [38] Maji BK, Jena H, Asuvathraman R. Electric conductivity and glass transition temperature (T<sub>g</sub>) measurements on some selected glasses used for nuclear waste immobilization. *Journal of Non-Crystalline Solids*. 2016; **434**:102-107
- [39] Berwal N, Dhankhar S, Sharma P, Kundu RS, Punia R, Kishore N. Physical, structural and optical characterization of silicate modified bismuth-borate-tellurite glasses. *Journal of Molecular Structure*. 2017;**1127**:636-644
- [40] Belova EV, Kolyagin YA, Uspenskaya IA. Structure and glass transition temperature of sodium-silicate glasses doped with iron. *Journal of Non-Crystalline Solids*. 2015; **423-424**:50-57
- [41] Hammad AH, Abdel-Hameed SAM, Margha FH. Effects of crystallization and microstructure on the dc electrical conductivity in the system xCuO-(70-x)MnO-30SiO<sub>2</sub>. *Journal of Alloys and Compounds*. 2015;**627**:423-429
- [42] Oueslati-Omrani R, Khattech I, Jemal M. Standard formation enthalpy of Na<sub>2</sub>O-ZnO-P<sub>2</sub>O<sub>5</sub> series glasses. *Chemistry Africa*. 2018;**1**:43-51
- [43] Cimek J, Stepien R, Klimczak M, Zalewska I. Developpement of thermally stable glass from SiO<sub>2</sub>-Bi<sub>2</sub>O<sub>3</sub>-PbO-ZnO-BaO oxide system suitable for all solid photonic crystal fibers. *Optical Materials*. 2017;**73**:277-283
- [44] Jlassi I, Sdiri N, Elhouichet H, Ferid M. Raman and impedance spectroscopy methods of P<sub>2</sub>O<sub>5</sub>-Li<sub>2</sub>O-Al<sub>2</sub>O<sub>3</sub> system doped with MgO. *Journal of Alloys and Compounds*. 2016;**645**: 125-130
- [45] Videau JJ, Flem L. Les verres phosphates de la spécificité de l'atome de phosphore à la formation, la structure, et la durabilité chimiques de phosphates vitreux. *Institut de chimie de la matière condensée de Bordeaux*; 27 October 2010. HAL Id: Cel-00530128
- [46] Montagne L, Palavit G, Dalaval R. 31P NMR in (100-x)NaPO<sub>3</sub>-xZnO glasses. *Journal of Non-Crystalline Solids*. 1997;**215**:1-10
- [47] Montagne L, Palavit G, Delaval R. Effect of ZnO on the properties of (100-x)NaPO<sub>3</sub>-xZnO glasses. *Journal of Non-Crystalline Solids*. 1998;**223**:43-47
- [48] Zotov N, Schlenz H, Brendebach B, Modrow H, Hormes J, Reinauer F, et al. Effects of MnO doping on the structure of sodium metaphosphate glasses. 2003; **58a**:419-428